# 2 CRITICAL STUDY ON PILED RAFT FOUNDATION

## 2.1 General

The critical study on piled raft foundation can be done using experimental method, numerical method or from the review of case studies on piled raft foundation. In this chapter, the experimental development made by various researchers is described in details in section 2.2. The developments on piled raft foundation topic through numerical studies are discussed in section 2.3 of this chapter. Various studies (observations) made by some researchers has been covered in section 2.4.

## 2.2 Experimental Developments

Numerous experimental findings that evaluate the performance of pile groups under various loading and soil conditions are reported in the literature (e.g., Al-Mahdi 2004, Lee and Chung 2005, Al-Mahdi 2006). Additionally, a number of small-scale tests have been carried out to examine the behaviour of piled raft foundations, and the results are summarized as follows.

Through a series of experiments on shallow footing, pile group, and piled raft under the same soil conditions, **Akinmusuru (1980)** showed that the bearing capacity of the piled raft foundations exceeds the sum of the bearing capacity of the raft and pile group. Further examples showed that the raft's bearing capacity in the piled raft foundation is comparable to that of a shallow footing. The following empirical relationship was suggested for determining the piled raft carrying capacity based on these observations:

$$Q_{PR} = \alpha' Q_{PG} + Q_R \qquad (2\text{-}1)$$

where, $Q_{PG}$ is the pile group's ultimate capacity, $Q_R$ is the raft's ultimate capacity, and $\alpha'$is the pile sharing factor that considers the influence of pile-soil-raft interaction on pile group ultimate capacity. It was demonstrated that $Q_{PR}$ is always greater than the sum of $Q_{PG}$ and $Q_R$ and decreases as pile length increases. He also showed how pile length and raft shape affect piled raft load sharing. Experiment results on a single piled raft unit (Figure 2-1) demonstrated that increasing the raft width significantly increases the raft share; however pile length has little effect on load sharing.

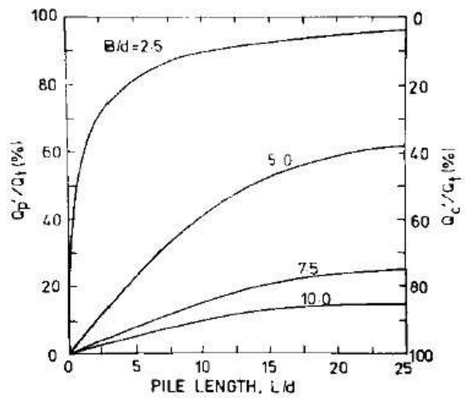


Figure 2-1: Load sharing between single pile and cap ( after Akinmusuru,1980)

**Wiesner and Brown (1980)** conducted an experimental study on models of raft foundations in an over consolidated clay to investigate the validity of methods based on elastic continuum theory for predicting the behaviour of the piled-raft foundation subjected to vertical loading. In this study, measurements of settlements, strains and bending moments in the raft were made and were observed that predictions of theory which was based on the assumption that soil is a linearly elastic continuum can provide acceptable predictions for the behaviour of piled-raft foundations.

**Liu et al. (1985),** conducted field studies on piled raft foundations in sand and reported that block failure does not occur for groups of bored piles in sand. For determining piled raft carrying capacity, the following empirical equation was proposed:

$$Q_{PR} = n(\beta_s \delta_s Q_{ss} + \beta_b \delta_b Q_{sb}) + Q_R \qquad (2\text{-}2)$$

where, $Q_{PR}$ = the ultimate capacity of piled raft foundation; $n$ = number of piles in the group; $Q_{ss}$ = shaft capacity of single pile; $Q_{sb}$= base capacity of single pile

$Q_R$ = raft ultimate capacity; $\delta$ and $\beta$ = coefficients represent pile-soil-pile and pile-soil-raft interaction respectively with subscript "s" stands for shaft capacity and subscript "b" stands for base capacity of pile.

**Cooke (1986)** provided the findings of piled-raft foundation model tests. He compared piled-raft foundation behaviour to that of the un-piled raft and free-standing piled group. Cooke

(1986) observed that the load distribution between piles in piled raft foundations was affected by pile number and spacing. He found that the settlement at the center of the raft foundation was greater than at the raft's edges.

**Phung (1993)** carried out field test in loose to dense sand and found that raft-pile interaction is the governing factor for pile raft behaviour, which causes an increase in skin friction of piles due to contact pressure of raft on soil.

**Horikoshi and Randolph (1996)** studied the settlement of piled-raft foundations on clay soil by conducting centrifuge experiments on piled-raft foundation models. They discovered that even a tiny group of piles might greatly lessen the raft's differential settlement. This study showed that a modest cap on a single pile might considerably boost the system's bearing capacity. Horikoshi et al. (2003) carried out centrifuge tests on piled-raft foundation models on sand soil that were exposed to vertical and horizontal loading. They investigated the effect of pile head connection rigidity on the behaviour of piled-raft foundations. This study found that as the cap comes into contact with soil, the confining stress surrounding the pile increases, increasing the pile's capacity. According to Horikoshi et al. (2003), the ultimate horizontal capacity of a piled-raft is greater than that of an un-piled raft.

**Conte et al. (2003)** conducted an experimental investigation using centrifuge tests to investigate the effect of raft and pile geometry modification on the rigidity of piled-raft foundations. They discovered that increasing the aspect ratio parameter, $R_M$ as provided by equation (2-3), increases the rigidity of piled-raft foundations.

$$R_M = \frac{A_R}{A_g}\sqrt{\frac{n * s}{L}} \qquad (2\text{-}3)$$

where, $A_R$= raft area; $A_g$= pile group area; $n$= number of piles; $s$= pile spacing; $L$= pile length

**Cao et al. (2004)** conducted experimental testing in plane-strain conditions to validate the usefulness of disconnected piles in decreasing raft settlement. In this study, the model raft was built on sand with a relative density of 70%, and numerous factors such as raft rigidity, pile length, pile arrangement, and pile number were changed. The testing results showed that unconnected piles beneath the raft are effective at preventing settlement and can carry up to 30% of the applied load on the raft at high pressures (Figure 2-2).

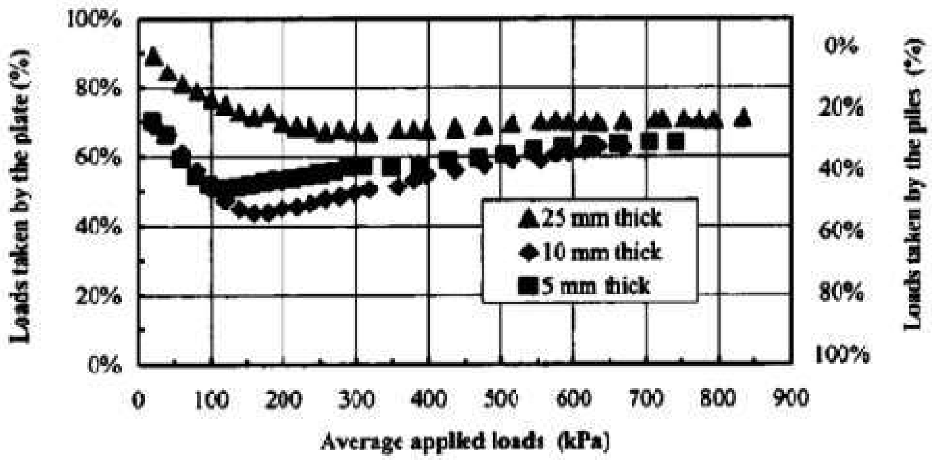


Figure 2-2: Fraction of loads taken by plates and piles for 500mm long piles (after Cao et al., 2004)

**Lee and Chung (2005)** conducted small scale model experiments on a single isolated pile, a single-loaded pile in a pile group, an un-piled footing, a freestanding pile group, and a piled raft. All of the pile groups in this study was made up of nine (3 × 3) piles driven into a compact sand deposit (Figure 2-3). The testing results indicated that contact between the raft and the underlying soil increases the skin friction of the piles as a function of pile spacing and pile position (Figure 2-4). The raft share in piled raft foundations was also shown to be comparable to un-piled raft behaviour.

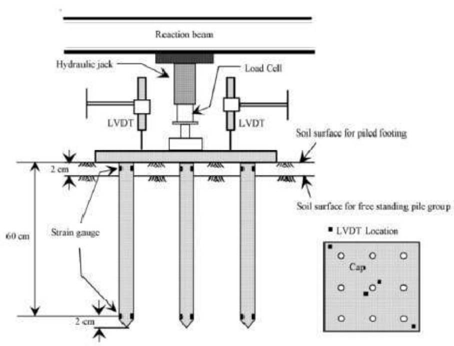


Figure 2-3: Schematic of test setup (after Lee and Chung, 2005)

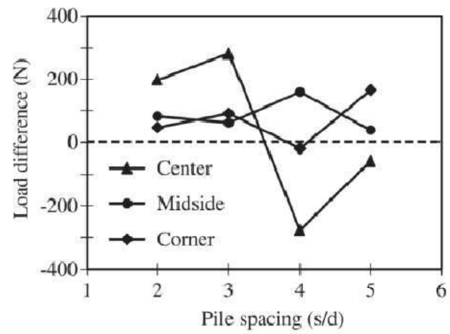


Figure 2-4: Difference in shaft friction between piles in free standing pile group and piled footing at the settlement of 3 mm or post-yield condition (after Lee and Chung, 2005)

**Fioravante et al. (2008)** published the findings of comprehensive centrifuge tests modeling a rigid circular piled-raft on sand soil to aid in the research of piles as settlement reducers and to quantify load sharing between the raft and piles. They discovered that when the number of piles increases, raft settlement reduces. The results demonstrated that displacement piles are more successful than non-displacement piles in reducing raft settlement. Fioravante et al. (2008) discovered that the raft's contribution begins as the piles approach their maximum capacity. They also noticed that piled-raft stiffness increased with the increase in the number of piles supporting the raft.

**Balakumar Venkatraman (2009)** conducted 1 g model tests on small-scale models to understand the load sharing and settlement reduction behaviour of circular piled raft resting on sand. The parameter analyzed were diameter, length and number of piles. The load-settlement response curves obtained analyzed and characterized. The characteristic response exhibited three phase behaviour irrespective of pile parameters and density of sand. The stiffness of piled raft system in the third phase is almost equal to raft-soil stiffness, which indicates that, piles perform essentially reducer rather than load sharing members. Finite element analysis for soil compares well with the experimental findings. At lower settlements piles share more load whereas raft shares higher load with increase in settlement.

**Phung Duc Long (2010)** endeavored to deepen the understanding of the load-transfer mechanism and load-settlement behaviour of a piled raft foundation in non-cohesive soil. The study also focused on the interaction between the piles, the cap, and the soil, with particular attention to the settlement-reducing effect of the piles. Three distinct series of large-scale model experiments (designated T1, T2, and T3) were carried out (Figure 2-5). Each test series included four separate tests on a shallow footing/cap (denoted as C), a single pile (S), a free-standing pile group (G), and a piled raft foundation (F) under identical soil conditions and geometry, as shown in Figure 2-5. The entire pile-cap-soil interaction of a piled footing in sand comprises interaction between the piles, known as pile-soil-pile interaction, as well as interaction between the piles and the pile cap (footing), known as pile-soil-cap interaction. The pile-soil-pile interaction is demonstrated by comparing the results of tests on free-standing pile groups with those on single piles, whereas the pile-soil-cap interaction is demonstrated by comparing the results of tests on piled footings with those on free-standing pile groups and on un-piled footings (cap alone).

Table 2-1 Summary of the large-scale field model tests, adopted from Phung Duc Long (2010)

| Test Series | Pile Group and Cap (Footing) | Sand $I_D$, % | Separate tests in one test series | Pile length $l_P$ (m) |
|---|---|---|---|---|
| T1 | square group of five piles<br>pile spacing $S$=4$b$<br>cap: 46cmx46cmx30cm | $I_D$ = 38% | T1C, shallow footing<br>T1S, single pile<br>T1G, pile group<br>T1F, piled footing | -<br>2.0<br>2.1<br>2.3 |
| T2 | square group of five piles<br>pile spacing $S$=6$b$<br>cap: 63cmx63cmx35cm | $I_D$ = 67% | T2C, shallow footing<br>T2S, single pile<br>T2G, pile group<br>T2F, piled footing | -<br>2.0<br>2.1<br>2.3 |
| T3 | square group of five piles<br>pile spacing $S$=8$b$<br>cap: 80cmx80cmx60cm | $I_D$ = 62% | T3C, shallow footing<br>T3S, single pile<br>T3G, pile group<br>T3F, piled footing | -<br>2.0<br>2.1<br>2.3 |

According to the test results, the carrying capacity of a piled raft (piled cap) foundation in non-cohesive soil $P_{ft}$ can be calculated as follows:

$$P_{ft} = n(\eta_{1s}\eta_{4s}P_{ss} + \eta_{1b}\eta_{4b}P_{sb}) + \eta_6 P_c \qquad (2\text{-}4)$$

where, $n$ = the number of piles in the group; $P_{ss}$ and $P_{sb}$ = the shaft and base capacities of a single reference pile, respectively; $P_c$ = the cap capacity. Table 2-2 represents additional symbols, with the indices "$s$" and "$b$" representing the (pile) shaft and base, respectively.

Table 2-2 Definitions of load efficiency factors, adopted from Phung Duc Long (2010)

| Symbols | Definition | comparison between |
|---|---|---|
| $\eta_1$ | $P_{gr}/nP_s$ | free-standing pile group and single pile |
| $\eta_4$ | $P_{fp}/P_{gr}$ | piled footing and free-standing pile group |
| $\eta_6$ | $P_{fc}/P_c$ | piled footing and shallow footing |

By comparing the load per pile in a free-standing pile group with that of a single pile at a certain settlement, such as $s$ = 10 mm, the efficiencies $\eta_{1s}$ and $\eta_{1b}$, which show the influence of the pile-soil-pile interaction on the pile shaft and base capacities, may be determined. For moderately dense to dense sand, they considered the efficiency $\eta_{1b}$ is unity, while for loose sand, it was considered more than unity.

Tests on piled footings done according to the second test protocol could clearly detect the efficiencies $\eta_{4s}$ and $\eta_{4b}$, which reveal the influence of the pile cap interaction on the pile shaft and base capacities. They consider $\eta_{4b}$ as unity for piles that are long enough ($L_p$ > 2.5$B_c$, where $L_p$ is the pile length and $B_c$ is the cap width). The efficiency $\eta_6$ represents the impact of the pile-cap-soil contact on cap capacity, and it ranged from 1.0 for loose sand to 0.9 for medium dense to dense sand.

From the test result, they suggested that a practical procedure of design of piled footing in sand can be carried out with the steps below:

1) To estimate the load taken by the cap (or unpiled raft) without causing excessive settlement. This load is equal to that can be taken in the cap in the piled raft footing $P_{cap}$;

2) To estimate the load taken by the piles $P_{piles} = P_{total} – P_{cap}$, where $P_{total}$ is the total applied load;

3) To determine the number of piles: As the piles are very close to failure state, the number of piles can be calculated as: $n = P_{piles} /P_s$, in which $P_s$ is ultimate capacity of a single pile.

In Step 1, the load-settlement relationship for the raft/footing without piles is evaluated using any available method for shallow footings. The Load carried by the cap can be selected at a predetermined (allowable) settlement level. The piles will carry the remaining load in Step 2. If the pile-soil-pile interaction doesn't know, factor $\eta_1$ and the pile-cap interaction factor $\eta_4$, can be taken as unity in Step 3. Furthermore, the number of piles can be estimated by dividing the load carried by pile group by the failure or creep load of a single pile. This is prudent because the pile shaft resistance increases significantly under cap-soil contact pressure.

The pile-soil-raft interaction governs piled raft behaviour through pile shaft capacity expansion; they found that the recorded pile share in a piled raft footing was much greater than the carried load by a free standing pile group in identical soil condition; pile position had no significant impact on the amount of the carried load by the pile in a piled raft system (Figure 2-6); prior to the piles failure, the majority of applied load was absorbed by the pile and was carried by the pile. In a piled raft footing, the raft's load-settlement behaviour was similar to that of a corresponding shallow foundation.

**El Sawwaf (2010)** examined connected and disconnected displacement piled raft footings under axial load and overturning moment (Figure 2-7). This study evaluated the effects of pile length, pile number, relative density of sand, and load eccentricity on the load-settlement behaviour of piled raft. The experiments were carried out at three distinct relative densities: 35%, 55%, and 80%. The following are the study's conclusions: the effectiveness of the piled raft system is affected by the load eccentricity ratio, pile layout, and relative density. Increasing the number of piles could only reduce settlement until a particular value was reached; the biggest improvement in raft behaviour was noticed when the sand was dense and the piles were attached to the raft (Figure 2-8). The study findings demonstrated that the use of short piles positioned near the edge of the raft effectively reduces both raft settlement and tilt while simultaneously increasing the strain borne by the raft. According to El Sawwaf (2010), the efficacy of short piles for increasing the performance of piled-raft foundations is dependent on pile configuration and load eccentricity ratio.

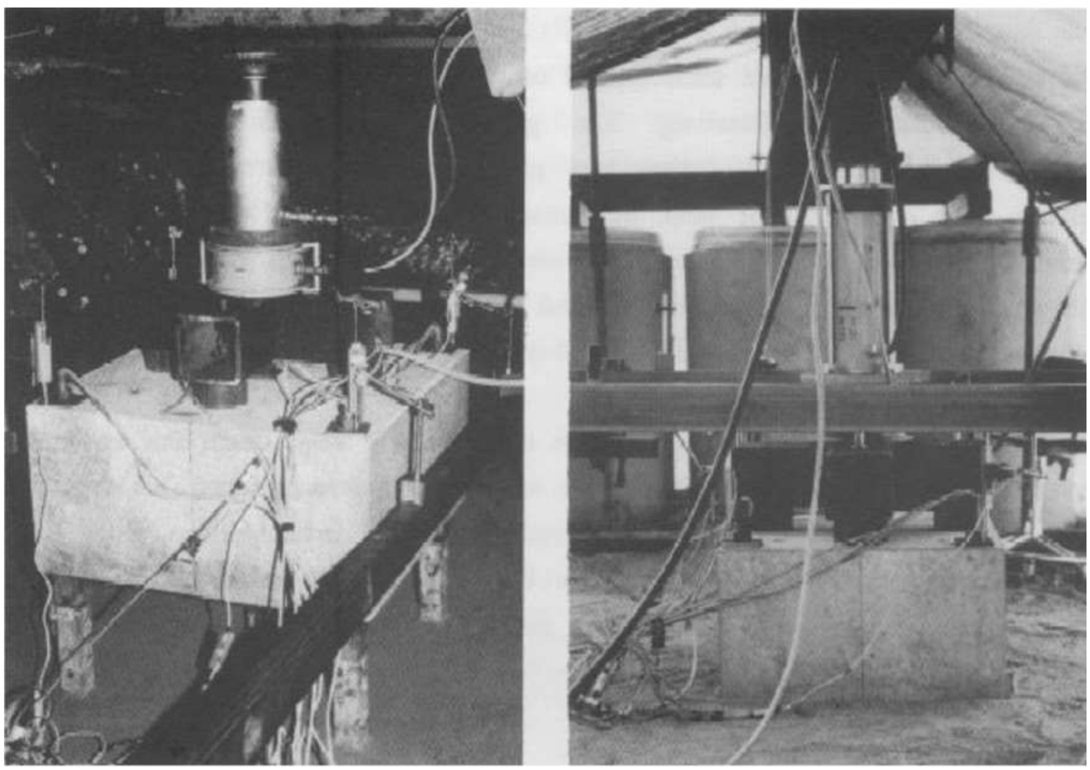

(a) (b)

Figure 2-5: Field large-model tests set up: (a) Test on a free-standing pile group; (b) Test on a piled footing with the cap in contact with soil ( after Phuong , 2010)

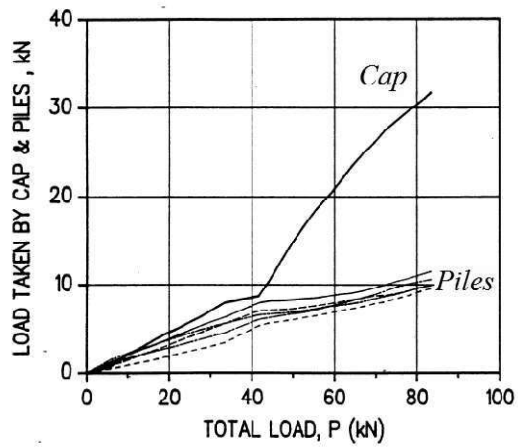


Figure 2-6 : Load share between cap and individual piles when the sand density and pile length are 38% and 2.3m respectively (after Phuong , 2010)

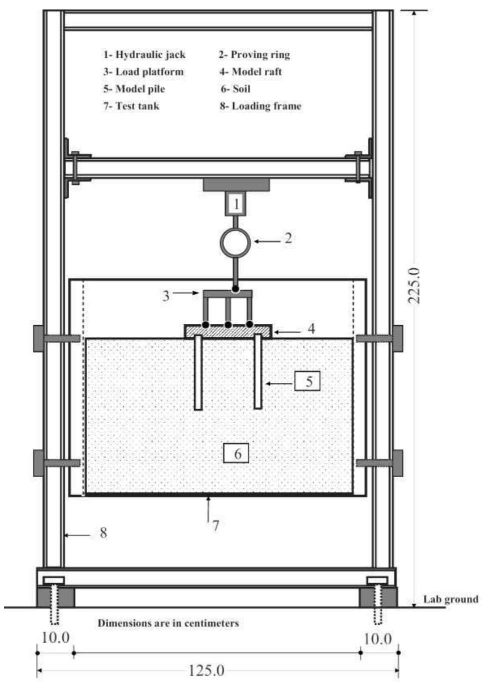


Figure 2-7: Schematic view of the experimental apparatus (after El Sawwaf , 2010)

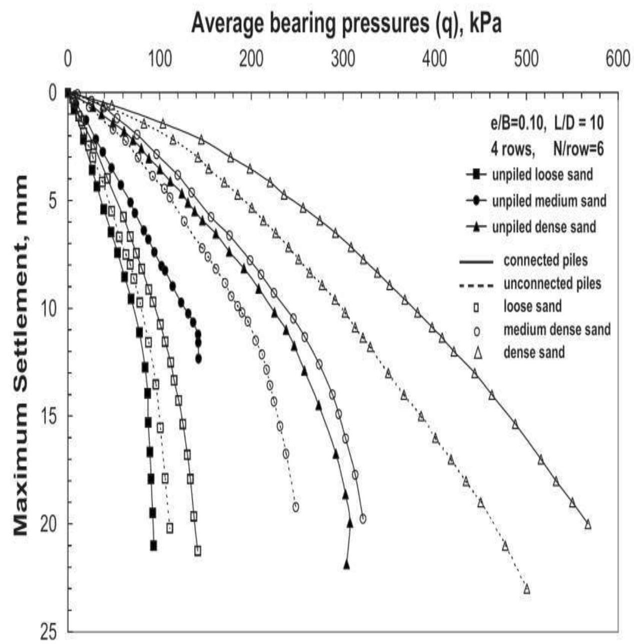


Figure 2-8 : Variation of average bearing pressures versus maximum settlement for different relative densities of sand (after El Sawwaf , 2010)

**Fioravante and Gritti (2010)** performed a centrifuge test on piled raft foundation in sandy soil and found that piles transfer the load from raft to wider and deeper volume of soil hence proved piles act as settlement reducer and also observed that sharing of load between pile and raft is related to stiffness of pile- soil system.

**Matsumoto et al. (2010)** used an experimental examination on piled-raft foundation models subjected to vertical and horizontal loads to evaluate the influence of pile head connection to the raft on the performance of piled raft foundations. They discovered that the pile head connection condition has no effect on the vertical loading behaviour of piled-raft foundations; however the horizontal load proportion borne by the raft decreases as the pile head connection becomes less stiff.

**Beren Yilmaz (2010)** carried out experimental research to observe the settlement behaviour of piled raft foundation system on clay. They used an aluminum model raft measuring 50 × 50 × 10 mm and brass model piles measuring 2 mm in diameter for preparing model piled raft foundation. They performed the experiments on same foundation soil by changing number of piles (16 to 49). It was concluded that placing piles under the raft greatly lowers settlement of foundation as compared to unpiled raft. However, the experiments also produced another significant finding that decrease in the settlement of piled raft foundation gets smaller when the pile count rises even higher. In other words, the settlement was not significantly impacted by an increase in the number of piles. In this research, an analytical settlement analysis proposed by Clancy and Randolph (1993) had been used.

Based on experimental studies and the analytical calculations, they concluded the following points:

The design of combination systems such as piled raft foundations and settlement reduction piles should be based on a predetermined maximum permissible settlement.

• The ideal number of piles for each design situation should be found by a trial and error approach depending on the tolerable settlement.

• The allocation of loads between the pile and the raft must undergo meticulous examination, and the outcomes should be integrated into settlement analyses. In scenarios where settlement-reducing piles are employed, it is possible for the factor of safety against pile bearing capacity to approach or even reach unity. However, this does not necessarily indicate that the system has become unsafe.

As the number of piles increased, the reduction in settlement did not, and the settlement curve tends to behave as a straight line beyond a certain point. In other words, there is an optimal amount of piles that should be placed beneath the raft for each design. This results in cost savings and a quicker building time.

**Giretti (2010)** investigated the behaviour of rigid raft on settlement reducing piles subjected to axial loading using two series of centrifuge tests. The first set of experiments were carried out on a rigid circular raft supported by either displacement or non-displacement piles and laying on a bed of fully saturated loose sand ($D_r$ = 30%). The testing programme included raft and piled raft experiments with 1, 3, 7, and 13 piles (Figure 2-9). The model raft had an 88 mm diameter and a 15 mm thickness. The close ended and free headed model piles used in these testing had a diameter of 8 mm and a length of 160 mm. The centrifuge test findings demonstrated that piles reduce settlement and that the number of displacement piles required to minimize settlement to an acceptable level is less than that of non-displacement piles (Fioravante et al. 2008). Figure 2-10 depicts the changes in load sharing vs. settlement for several piled raft layouts. Load sharing fluctuates non-linearly with the settlement ratio ($W/d_r$), and pile share increases as the number of piles increases.
The second set of centrifuge experiments were conducted in two scenarios in which a rigid raft was either linked or separated from the driven piles in the dry sand deposit ($D_r$ = 60%). The testing program included raft, single pile, and piled raft tests with one, four, and nine displacement piles (Figure 2-11). The model raft had a 115 mm width and a 25 mm height. The model piles used were close ended and free headed, with diameters of 8 mm and lengths of 292 mm. According to the test results, connected piles work as settlement reducers by shifting the imposed load on their heads to deeper soil volume, whereas non-connected piles primarily serve as soil reinforcement. Furthermore, the pile-soil-raft interaction produces negative skin friction on the upper part of pile shafts, and the stiffness modulus of connected piled raft decreases by settlement until it reaches the raft stiffness at pile group failure point (Fioravante, 2011).

**Dr.Mosa J. Al-Mosawi et al. (2011)** did experimental study to investigate the behaviour of piled raft system in sandy soil. They prepared a small scale "Prototype" model and tested in a sand box with load applied to the system through a compression machine. The settlement was measured at the centre of the raft, strain gages were used to measure the strains and calculate the total load carried by piles. They tested four configurations of piles (2×1, 3×1, 2×2 and 3×2) in the laboratory, in addition to rafts with different sizes. The effects of pile length, pile diameter, and raft thickness on the load carrying capacity of the piled raft system included in the load – settlement presentation. They found that the percentage of the applied load carried by piles to the total applied load of the groups (2×1, 3×1, 2×2 and 3×2)with raft thickness of 5 mm, pile diameter of 9 mm, and pile length of 200 mm was 28%, 38%, 56% and 79% respectively. The percentage of the load carried by piles was increased with the increase of number of piles.

**Qaissy et al. (2013)** performed experimental study on two different scale models with the same $L/D_p$ (Embedment length to pile diameter ratio) and $L/B_r$ (Embedded length to raft width ratio) to achieve the scale effect for the large scale model and plane strain condition for the small scale model. They found that the percentage of the load carried by raft to the total applied load of the experimental model in the case of four piles with raft was ranged between 60.6 - 64.8%.

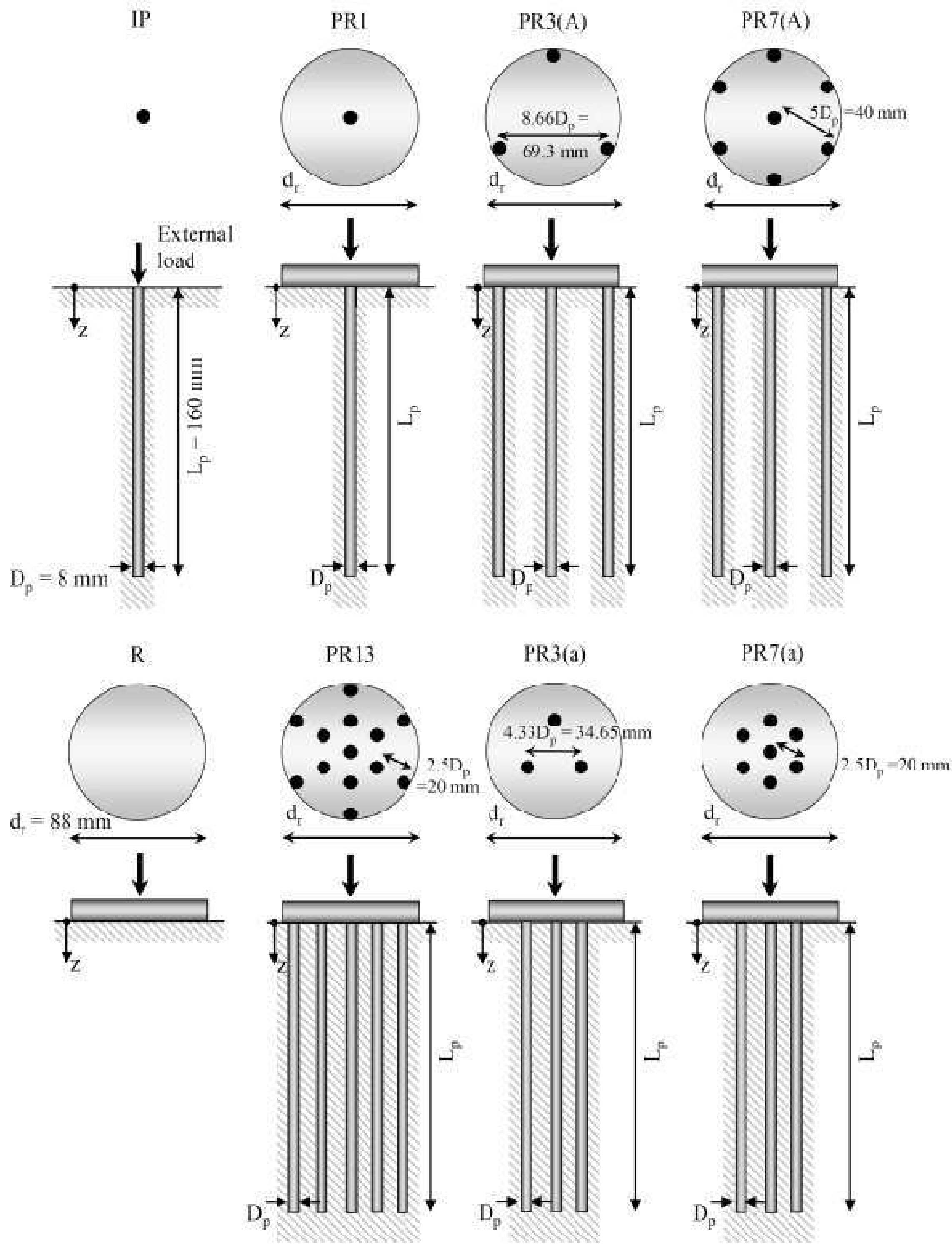


Figure 2-9 : Piled raft configurations in the centrifuge tests (after Giretti, 2010)

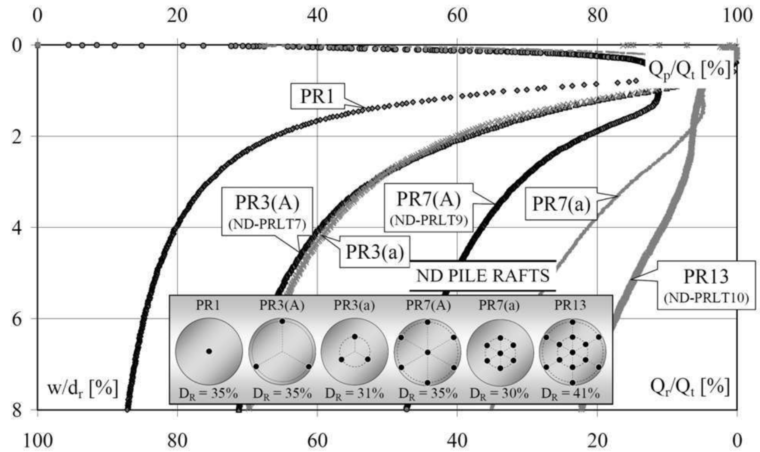


Figure 2-10 : Variation of load sharing versus raft relative settlement (settlement of piled raft over raft diameter) (after Giretti, 2010)

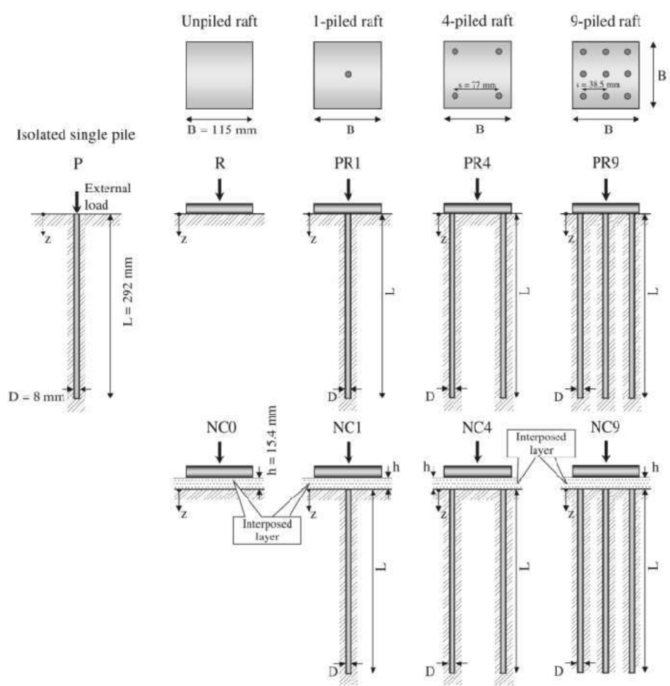


Figure 2-11 : Schematic view of model foundations in the series #2 of centrifuge tests (after Fioravante and Giretti, 2010)

**El-Garhy et al. (2013)** conducted small scale tests to investigate the behaviour of piled raft foundations in sand. The pile spacing was held constant in the test program ($S = 3.5\ d_p$), while the pile length; number of piles, and raft thickness were varied. The test findings showed that: raft thickness and pile length had insignificant influence on piled raft load sharing (Figure 2-12 and Figure 2-13); increasing the number of piles results in a greater share of load borne by each individual pile when pile spacing and raft size were constant (Figure 2-13).

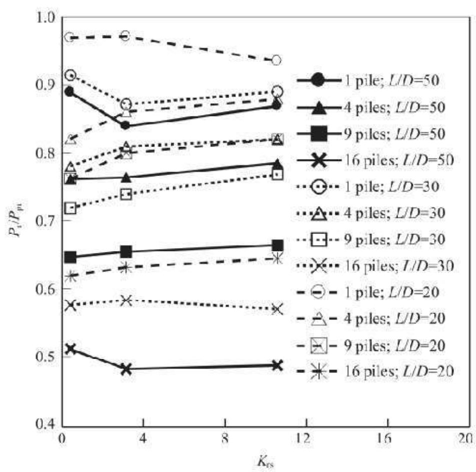


Figure 2-12 : Variation of raft share versus raft relative stiffness for piled raft with different number of piles and slenderness ratios ( after El-Garhy et al., 2013)

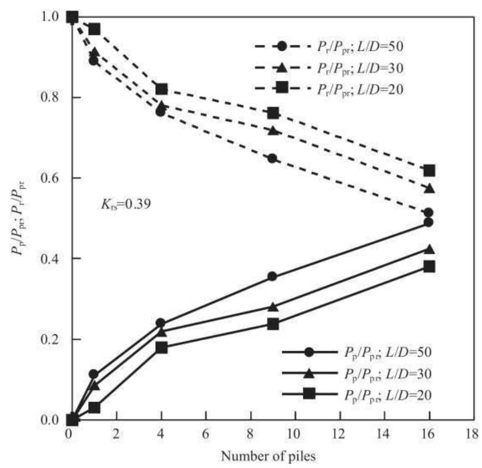


Figure 2-13 Load sharing of a piled raft with different number of piles and also various slenderness ratio ( after El-Garhy et al., 2013)

**Juneja et al. (2013)** conducted 1g model tests to understand the effects of raft thickness, number and length of piles on the load shared by the piles. They computed load shared by the piles from the model tests as well as theoretically in terms of piled raft coefficients.

The piled raft coefficient, $\alpha_{PR}$ shows the load shared by the piles in piled raft is given as

$$\alpha_{PR} = \frac{\sum Q_{p,t}}{Q_{PR,ult}} \tag{2-5}$$

where, $Q_{p,t}$= pile resistance

$Q_{PR,ult}$= total resistance of the foundation

Theoretically, the coefficients $\beta_{PR}$ and $\xi_{PR}$ were been also determined. The coefficients were been established in accordance with De Sanctis and Mandolini.

$$\beta_{PR} = \frac{\sum Q_{PR,ult}}{Q_{G,ult}} \tag{2-6}$$

where, $Q_{PR,ult}$= ultimate load capacity of a piled raft, $Q_{G,ult}$= ultimate load capacity of a pile group. $\beta_{PR}$ shows the contribution of raft in the load bearing.

$$\xi_{PR} = \frac{Q_{PR,ult}}{Q_{UR,ult} + Q_{G,ult}} \tag{2-7}$$

where, $Q_{PR,ult}$ = ultimate load capacity of a piled raft, $Q_{G,ult}$ = ultimate load capacity of a pile group, $Q_{UR,ult}$ = ultimate load capacity of unpiled raft, $\xi_{PR}$ shows the ultimate capacity of piled raft as a percentage of sum of ultimate capacities of raft and piles taken as separate components.

According to their observations, as the load increased, the overall load shared by the piles decreased. For a larger number of piles, the load shared by the piles increased with the length of the central pile and was roughly the same for different raft thicknesses. A large contribution of raft was obtained when fewer piles were used. Except for the single piled raft, where raft contributes significantly, the values of $\beta_{PR}$ ranged from 1.9 to 2.9 in their testing. The findings agreed with those of Cook, who reported that $\beta_{PR}$ varied from 1.25 to 2.5 depending on the length, spacing, number of piles, and breadth of the raft. It was also found that in general the value of $\beta_{PR}$ i.e. the contribution of the raft decreases with the number of piles and length of piles. The values of $\xi_{PR}$ for all the tests were found to be in the range of 0.99 to 1. i.e, the governing failure in both the pile group and piled raft was individual failure rather than block failure. This means that the ultimate capacity of the piled raft was found to be at least 99% of the ultimate capacities of the raft and piles taken separately. Such values are high and they suggested computing $\xi_{PR}$ from experimental data.

**Patil et al. (2014)** performed experiments to study the behaviour of piled raft foundation system subjected to vertical load on dry sand. The experimental program included the model test on unpiled raft, raft supported by single pile, (2 × 2) and (3 × 3) pile groups with *L/d* ratio = 10 and spacing = *3d*. They concluded that the load bearing capacity of piled raft increased as the number of piles beneath the raft increased, Load improvement ratio increased at 10 mm and 20 mm settlement, as the number of pile increased. The raft thickness has insignificant effect on the settlement and the load sharing between piles and raft. The efficiency of piled raft foundation system in reducing settlement was minimal beyond a certain number of piles.

**Radhika et al. (2015)** did parametric study and numerical analysis of piled raft foundation on soft clay. Laboratory model tests were conducted on both unpiled and piled raft on soft clay. The model tests included the use of unpiled raft and piled raft of three configurations namely 1 × 1, 2 × 2 and 3 × 3 with varying *L/d* Ratio of pile 23, 27 and 30. The results proved that ultimate load had increased and the settlement had reduced which was expressed by Load Improvement Ratio *(LIR)* and Settlement Ratio (*SR*). A parametric study indicated that an increase in pile length and the number of piles results in a reduction in settlement. Among the tested footing models, the maximum pile length was 180 mm. A piled raft with a 3 × 3 configuration demonstrated a 67% increase in ultimate load and an 83% reduction in settlement compared to the same configuration with a pile length of 140 mm. The observed settlement values from the experimental study were compared with numerical modeling using PLAXIS 2D, and the results showed good agreement.

**Vakili (2015)** studied the load sharing mechanism of a piled raft foundation in sandy soil through small scale tests and three dimensional numerical analyses. Experiments were conducted to examine the effects of density in homogeneous and stratified soil, particle size distribution of sand, pile installation method, and raft width on load sharing behaviour of piled raft foundation. In clean Silica sand, experiments were carried out on a shallow footing, a single pile, and a single piled raft unit. They observed in small scale tests that soil density altered the load sharing mechanism of a displacement piled raft, with the pile share increasing in denser soil. They found that, in non-displacement piled rafts the load sharing was independent of soil density and particle size distribution had insignificant effects on piled raft behaviour. One of the non-displacement piled raft experimental tests was used to calibrate the 3D numerical model, which was then expanded into 2 × 2 and 3 × 3 piled raft foundations. For a given settlement ratio, the load sharing outputs of the aforementioned models were compared.

From the experimental and numerical results and a literature review, they analyzed that the load sharing of a non-displacement piled raft foundation in homogeneous sand is a function of two variables, $S/d_p$ (spacing to pile diameter ratio) and $W/d_r$ (settlement to raft width ratio) ratios, but independent of soil relative density, number of piles, and pile slenderness ratio. They used experimental studies on non-displacement piled raft foundations in medium sand to build the load sharing empirical model. The empirical design chart developed for pile spacing ranges from $3.5\ d_p$ to $6\ d_p$ under operating load are shown in Figure 2-14.

Furthermore, **Yamashita et al. (2011) and Sinha (2013)** demonstrated that the relationship between load sharing and pile spacing reaches a saturation point at spacing = $6d_p$, so they suggested to use the proposed load sharing curve at $S/d_p = 6$ for any pile spacing greater than 6. They proposed empirical curves for load sharing as shown in Figure 2-14 to Figure 2-18.

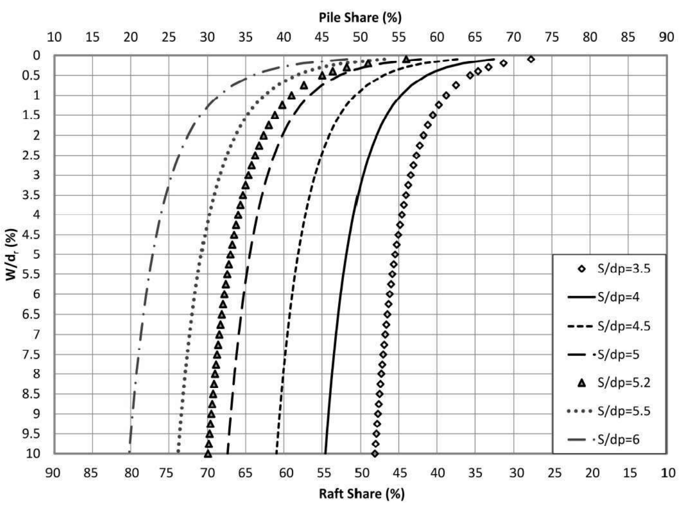


Figure 2-14 : The proposed empirical curves for estimating the load sharing of non-displacement piled raft in homogeneous sand as the function of $W/d_r$ and $S/d_p$ ( after Vakili, 2015)

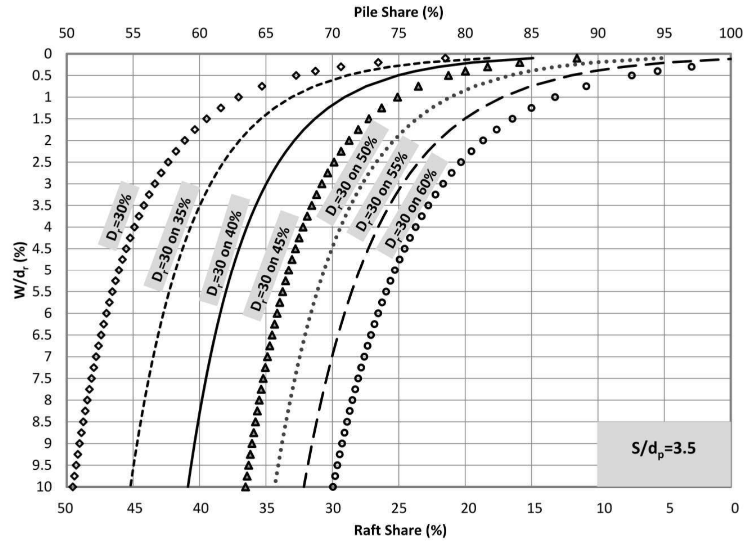


Figure 2-15 : Proposed empirical curves for estimating the load sharing of non-displacement piled raft in layered soil when the raft was founded on loose sand, and $S/d_p=3.5$ ( after Vakili, 2015)

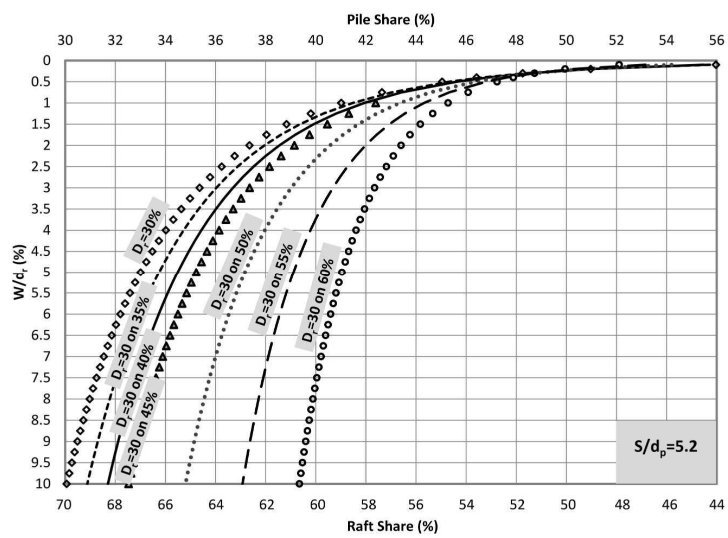


Figure 2-16 : Proposed empirical curves for estimating the load sharing of non-displacement piled raft in layered soil when the raft was founded on loose sand, and $S/d_p=5.2$ ( after Vakili, 2015)

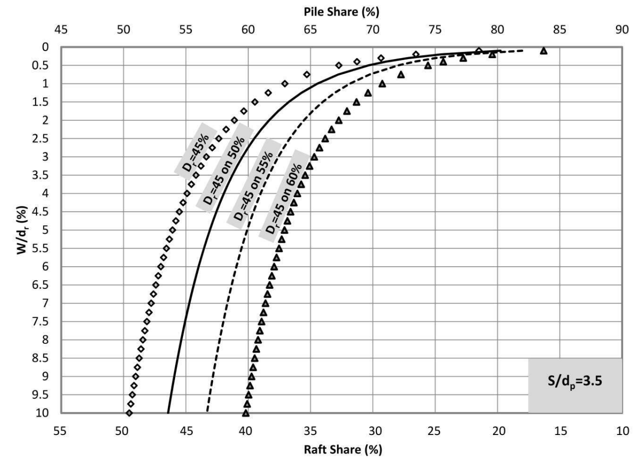


Figure 2-17 : Proposed empirical curves for estimating the load sharing of non-displacement piled raft in layered soil when the raft was founded on medium sand, and $S/d_p=3.5$ ( after Vakili, 2015)

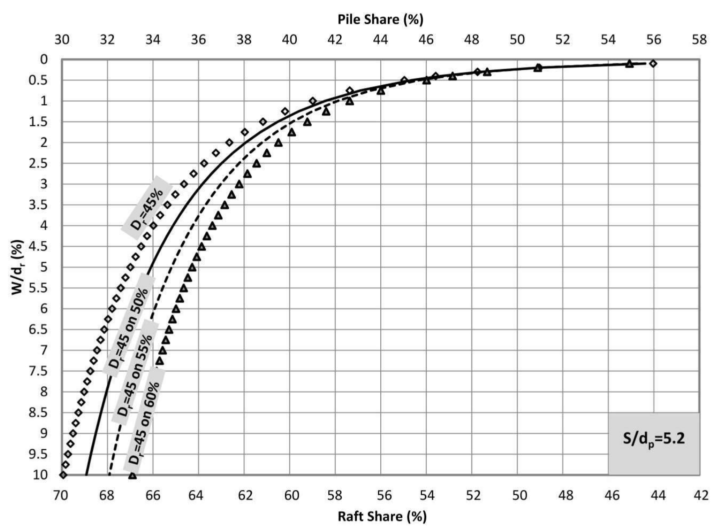


Figure 2-18 : Proposed curves for estimating the load sharing of non-displacement piled raft in layered soil when the raft was founded on medium sand, and $S/d_p=5.2$ ( after Vakili, 2015)

**Park and Lee (2015)** investigated the load responses and interaction effects of piled rafts embedded in sands. Several centrifuge load experiments were performed utilizing various model foundation types. In the tests, different types of piles, single piles, group piles, piled rafts, and unpiled rafts were used to examine the various interaction effects of piled rafts. They observed that for the early range of settlement, the load-settlement curves of piled rafts were comparable to those of group piles, and as settlement progressed, it became comparable to those of rafts. The interaction factors between pile groups, piles and rafts, and rafts and piles displayed state-dependent and nonlinear variations with settlement. Within the initial settlement range, the pile-to-raft and raft-to-pile interaction factors decreased, and with increasing settlement, it increased. The range of values for the raft-to-pile interaction factor was substantially smaller than the range for the pile-to-raft interaction factor. As opposed to single piles, piled rafts had different load responses and load transfer relationships, demonstrating that the effect of raft-to-pile interaction was more significant in the upper soil zone. They suggested that the mobilized factor of safety for rafts should always greater than the safety factor for piles and piled rafts due to the lower mobilized load-carrying capability of rafts.

**Elwakil et al. (2016)** conducted an experimental and numerical study, employing PLAXIS 2D, to investigate the behaviour of a piled raft system. This research delves into the rationale behind using piles as settlement reducers for raft foundations, as well as the behaviour of piled rafts embedded in sand. Small-scale model tests were conducted, focusing on the effects of pile length and alignment on the ultimate load capacity attained.

The factor $\beta$ is introduced and defined as

$$\beta = \frac{piled\ raft\ load}{pile\ load + raft\ load} = \frac{PR}{P+R} \tag{2-8}$$

Generally the ultimate capacity attained by piled raft models tested in this investigation had been expressed by the following equation:

$$Q_u = 0.036N + 0.7 \ \ for\ 0.67 \leq {}^{L}/_{B} \leq 2.67 \tag{2-9}$$

where, $Q_u$ is the ultimate load carried by the piled raft in kN and N is the number of piles.

$$PR \geq P + R \; at \; {}^{S}/_{B} = 0.7\% \qquad (2\text{-}10)$$

where, $PR$ =the piled raft load, $P$ = the piles load, P, and $R$ = raft load,

Following conclusions were highlighted in this study:

1. The load shared by the raft in piled raft foundation on sand was found around 39% of total load. The load shared by raft was increased as the length and number of the piles decreases.

2. The load carried by the piled raft is greater than the summation of the loads carried by the unpiled raft and the piles for each settlement ratio when *S/B* is less than or equal to 0.7%. It can be proposed to construct the piled raft at *S/B* = 0.7% for the optimal performance.

3. The maximum load achieved by the piled raft with 16 piles is 30% higher than the one with 4 piles.

4. Considering the size of settlements, the numerical model used in this study appears to operate in a very reasonable manner. This suggests that utilizing a plane strain model in PLAXIS 2D can save time compared to employing a more intricate three-dimensional model to obtain a preliminary result.

5. The finite element analysis improved comprehension of the piled raft soil system failure patterns. Additionally, it supported the findings of various researchers regarding the load transfer mechanism of an equivalent pier.

**Jamil et al. (2023)** carried out experimental and numerical studies on different small-scale models of piled raft foundations under vertical and lateral load. Small-scale models of the aluminum raft and galvanized iron (GI) hollow piles were tested under vertical and lateral loads in the experimental technique. For real-time load monitoring, vertical and lateral load cells were put on piles, while LVDTs were employed for displacement monitoring. PLAXIS 3D finite element software was employed in the numerical technique. A raft was classified as a plate element, and piles as embedded beams. Based on experimental and computational results, they discovered that vertical raft contact with soil had a direct link with lateral raft contribution. Because of the vertical load, a firm contact develops between the raft and the soil, resulting in a large lateral contribution. As a consequence, PLAXIS 3D was used to do a parametric analysis and it was discovered that vertical pressure was directly related to lateral raft resistance, whereas the other three parameters were inversely related. They found that as the number of piles increased from 1 to 13, the load shared by piles of piled raft foundation increased from 13% to 85% (Figure 2-19 and Figure 2-20).

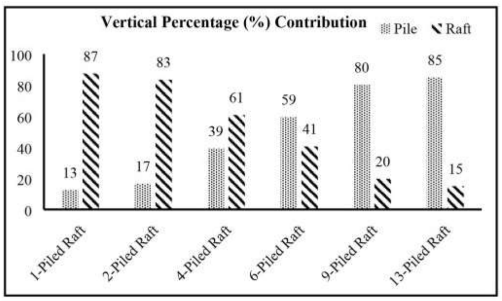


Figure 2-19 : Experimental results with *s/d = 6.67* and *s/d = 3.33* for 13 piled raft (after Jamil et. Al, 2023)

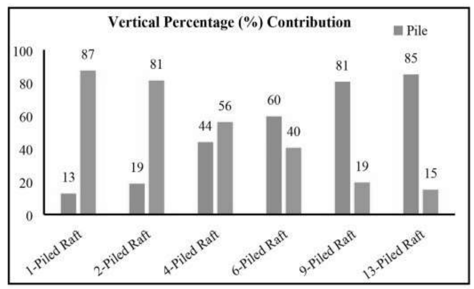


Figure 2-20 Numerical results with *s/d = 6.67* and *s/d = 3.33* for 13 piled raft (after Jamil et. Al, 2023)

## 2.3 Numerical/ Analytical Developments

For piled raft foundations, a number of analytical/numerical approaches have been put forth; some of these were compiled by Poulos and Davis (1980), Randolph (1983,1994), vanImpe and Clerq (1995), Burland (1995), Phung (2010), Lee et al. (2014), Alsanabani (2017), Garcia et al. (2019), and Bhartiyal (2020). All analytical/numerical techniques could be divided into four groups:

1) Simplified analysis method: This makes a number of assumptions about how the soil profile should be modeled and how the raft should be loaded.

2) Approximate computer–based method: The approximate computer-based methods comprise the following broad approaches:

• "Strip on springs" methods, where the piles are represented by appropriate stiffness springs and the raft is represented by a series of strip footings (e.g. Poulos, 1991);

• Approaches based on the "plate on springs" principle, in which the piles are represented by springs and the raft by plates (e.g., Clancy and Randolph, 1993; Poulos, 1994; Viggiani, 1998; and poulos and Georgiadis, 1998).

3) More rigorous computer–based method: The following are some of the most rigorous methods:

• Elastic theory is utilized to discretize the raft and the piles within the system using boundary element methods (e.g. Butterfield and Banerjee, 1971; Brown and Wiesner, 1975; Kuwabara, 1989; and Sinha, 1997).

• Techniques for the piles and the raft that combine boundary element and finite element analysis (Hain and Lee, 1978; Ta and Small, 1996; Franke et al., 1994; Russo and Viggiani, 1998)

• Simplified finite element analyses, which frequently entail modeling the foundation system as a plane strain problem (Desai, 1974) or an axi-symmetric problem (Hooper, 1974), as well as associated finite difference analyses utilizing the commercial software FLAC (e.g. Hewitt and Gue, 1994).

4) Accurate Numerical Method:

Two-dimensional (2D) numerical analyses,
Three-dimensional (3D) numerical analyses.

The simplified and numerical methods are discussed more below.

This makes a number of assumptions about how the soil profile should be modeled and how the raft should be loaded. Several simplified systems for analyzing piled raft foundations have been offered (e.g., Poulos and Davis 1980, Randolph 1994, Van Impe and Clerq 1995, and Borland 1995). Lee et al. (2014) provided a model for load-sharing determination that took into consideration the settlement-dependent variance in load-sharing behaviour more recently. Although this method is more advanced, the model's essential assumptions limit its applications. The Poulos-Davis-Randolph method, which is explained in the next section, is the most frequently accepted simplified method.

**Simplified analysis method:**

**Poulos-Davis-Randolph (PDR) Method**

The ultimate load capacity of a piled raft foundation can often be taken as the lesser of the following two values when analyzing vertical bearing capacity using simple approaches: (1) The total of the raft's ultimate capacities plus all of the piles, (2) The maximum capacity of a block containing the piles and the raft, plus the portion of the raft outside the piles' periphery.

There are different approaches for predicting stiffness, pile-raft interaction factors, settlement of a piled raft, and load sharing between the piles and raft component of a piled raft foundation.

**Randolph (1983)** presented a simplified approach for evaluating a piled raft foundation's load sharing. The approach was designed for a single piled raft unit with a floating pile coupled to a stiff circular cap and supported by an elastic semi-infinite mass. The stiffness of the piled raft evaluated using this method as follows:

The overall stiffness of piled raft system can be calculated as per **Clancy and Randolph (1993)** as below:

$$k_{pr} = \frac{(P_p + P_r)}{w_{pr}} = \frac{\left[k_p + k_r\left(1 - 2\alpha_{rp}\right)\right]}{\left[1 - \left(k_r/k_p\right)\alpha^2{}_{rp}\right]} \qquad (2\text{-}11)$$

$$P_p = \frac{\left[1 - k_r\left({}^{\alpha_{rp}}\!/_{k_p}\right)\right]}{\left({}^{1}\!/_{k_p}\right) - k_r\left({}^{\alpha_{rp}}\!/_{k_p}\right)^2} w_{pr} \tag{2-12}$$

$$P_r = \frac{\left[\left(\frac{k_r}{k_p}\right) - k_r\left({}^{\alpha_{rp}}\!/_{k_p}\right)\right]}{\left({}^{1}\!/_{k_p}\right) - k_r\left({}^{\alpha_{rp}}\!/_{k_p}\right)^2} w_{pr} \tag{2-13}$$

where,

$k_{pr} = overall\ stiffness\ of\ the\ piledraft\ system$

$P_p = Total\ load\ carried\ by\ pile\ group\ in\ combined\ foundation$

$P_r = total\ loadcarried\ by\ raft\ in\ combined\ foundation$

$k_p = overall\ stiffness\ of\ pile\ group\ in\ isolation$

$k_r\ = overall\ stiffness\ of\ raft\ in\ isolation$

$w_{pr} = overall\ piledraft\ settlement(\ for\ rigid\ raft\ w_{pr} = w_p = w_r)$

$\alpha_{rp} =\ Interaction\ factor\ of\ pile\ group\ on\ raft$

$\alpha_{pr} =\ interaction\ factor\ of\ raft\ on\ pile\ group$

$k_p$ can be calculated using the relationship between number of piles and stiffness of single pile (initial tangent of load settlement curve of single pile) $k_{p1}$ as mentioned by **Fleming et al. (1992)**

$$k_p = k_{p1} * (n)^{1-e} \tag{2-14}$$

where $n$ represents the number of piles and the exponent ranges between 0.3 and 0.5 for friction piles.

The equation proposed by (Sales, 2000) can be used to express pile stiffness:

$$k_{p1} = \frac{P}{\delta} \tag{2-15}$$

where $P$ is the load applied to the pile and δ is the displacement caused by the action of $P$ on the pile's top.

In the absence of pile load test data, the pile is modeled as a series of linear elastic springs, while the resistances at the toe and shaft are modeled as nonlinear springs expressing soil deformation.

As per Randolph, stiffness factor for the system is defined by using equation (2-16)

$$\alpha_{rp} = 1 - \frac{ln(n)}{ln\left({}^{2r_m}/_{d}\right)} \tag{2-16}$$

$$\alpha_{pr} = \alpha_{rp} \frac{k_r}{k_p} \tag{2-17}$$

where, $n$ = ratio of the circular raft diameter to the pile diameter

$r_m$ = a measure of the radius of influence of the pile

$$r_m = 2.5[\rho L(1 - \nu_s)] \tag{2-18}$$

$\rho$= the degree of homogeneity of the soil

$L$ = the pile length

$\nu_s$ = Poisson's ratio of the soil

For very slender piles, the pile length $L$ is replaced by a limiting effective pile length $L_e$which may be calculated according to Fleming et al. (1992)

$$L_e = 1.5\, d \sqrt{2(1 + \nu_s)\, {}^{E_p}\!/_{E_s}} \tag{2-19}$$

As per Clancy and Randolph (1993) the settlement of piled raft foundation can be calculated as below

$$\alpha_{rp} = \frac{k_p}{P_p}\left(w_{pr} - \frac{P_r}{k_r}\right) \tag{2-20}$$

$$\alpha_{pr} = \frac{k_r}{P_r}\left(w_{pr} - \frac{P_p}{k_p}\right) \tag{2-21}$$

**Poulos (2001)** discussed the design process for a piled raft, considering a three-stage process.

(a) A preliminary stage to determine whether utilizing a piled raft is feasible; and the necessary number of piles to meet design requirements.

(b) A second stage to determine the locations where piles are needed and their overall characteristics.

(c) A final comprehensive design step to determine the ideal number, placement, and configuration of the piles and to compute the loads and moments of the piles as well as the exact distributions of settlement, bending moment, and shear in the raft.

**(a) Stage of preliminary design:**

In the early stage, the performance of a raft foundation without piling must be evaluated. Conventional approaches can be used to estimate vertical and lateral bearing capacity, settlement, and differential settlement. If the raft alone supplies only a little part of the needed load capacity, the foundation will almost certainly need to be planned using the conventional methodology as a pile foundation. If, on the other hand, the raft alone has appropriate or nearly adequate load capacity but does not meet the settlement or differential settlement criteria, it may be feasible to consider the use of piles as settlement reducers or the 'creep piling' strategy.

The ultimate load capacity can often be taken as the lesser of two values when calculating vertical bearing capacity: (i) the total of the ultimate capacities of the raft plus all the piles; (ii) the ultimate capacity of a block including the piles and the raft, plus the section of the raft outside the piles' periphery.

A technique similar to that presented by Poulos and Davis (1980) can be used to estimate the load-settlement behaviour. However, a valuable addition to this method can be developed by employing Randolph's (1994) simple way of predicting the load sharing between the raft and the piles.

Randolph's definition of the pile problem is depicted in Figure 2-21. The stiffness of the piled raft foundation can be determined through his method as follows:

As per Poulos (2001) the stiffness of piled raft can be calculated as

$$k_{pr} = \frac{(P_p + P_r)}{w_{pr}} = \frac{[k_p + k_r(1 - \alpha_{cp})]}{[1 - k_r k_p \alpha^2{}_{cp}\ ]} \qquad (2\text{-}22)$$

$\alpha_{cp}$= The raft – pile interaction factor

$$\alpha_{cp} = 1 - \frac{ln\left({}^{r_c}/_{r_0}\right)}{ln\left({}^{r_m}/_{r_0}\right)} \qquad (2\text{-}23)$$

where, $r_c$ = Average radius of pile cap (corresponding to an area equal to the raft area divided by number of piles); $r_0$ = radius of pile;

$$r_m = 0.25 + \xi[2.5 * \rho L(1 - \nu_s) - 0.25]L \qquad (2\text{-}24)$$

where,

$\xi = {}^{E_{sl}}/_{E_{sb}}$; $\rho = {}^{E_{sav}}/_{E_{sl}}$ ; $\nu_s$ =Poisson's ratio of soil; $L$= pile length; $E_{sl}$ = soil Young's modulus at level of pile tip; $E_{sb}$= soil Young's modulus of bearing stratum below pile tip; and $E_{sav}$ =average soil Young's modulus along pile shaft. The raft stiffness $k_r$ can be calculated using elastic theory, such as the solutions of Fraser and Wardle (1976) or Mayne and Poulos (1999). Elastic theory can also be used to estimate pile group stiffness, as detailed by Poulos & Davis (1980), Fleming et al. (1992), or Poulos (1989). In the latter situation, the single pile stiffness is calculated using elastic theory and then multiplied by a group stiffness efficiency factor determined roughly from elastic solutions.

As per **Poulos (2001)** the proportion of the total applied load carried by the raft is

$$X = \frac{P_r}{P_t} = \frac{[k_r(1 - \alpha_{cp})]}{k_p + k_r(1 - \alpha_{cp})} \qquad (2\text{-}25)$$

where, $P_r$ = load carried by the raft; $P_t$= total applied load.

The above equations can be used to develop a tri-linear load-settlement curve as shown in Figure 2-22. First, the stiffness of the piled raft can be computed from equation (2-22) for the number of piles being considered. This stiffness will remain operative until the pile capacity is fully mobilized. Making the simplifying assumption that the pile load mobilization occurred simultaneously, the total applied load, $P_1$, at which the pile capacity is reached, is given by:

$$P_1 = \frac{P_{up}}{1 - X} \tag{2-26}$$

where, $P_{up}$ = ultimate load capacity of the piles in the group; $X$ = proportion of load carried by the raft (Equation (2-25)).

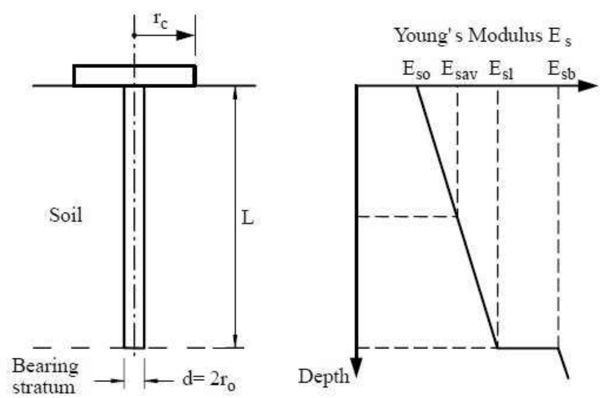


Figure 2-21: Simplified representation of a pile-raft unit (after Poulos, 2001)

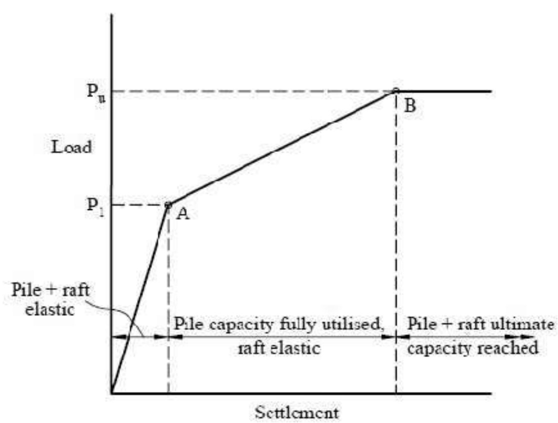


Figure 2-22 : Simplified load-settlement curve for preliminary analysis of piled raft foundation (after Poulos, 2001)

Beyond that point (Point A in Figure 2-22), the stiffness of the foundation system is that of the raft alone ($k_r$), and this holds until the piled raft foundation system's ultimate load capacity is reached (Point B in Figure 2-22). The load-settlement relationship becomes horizontal at that point.

According to **Randolph (1994),** and mentioned by **Garcia et al. (2019)** stiffness is the ratio between a particular load and the displacement it causes. Thus, up to point A of the Figure 2-22 graph, the settlement of a foundation can be given by:

$$w = \frac{P}{k_{pr}} \qquad (2\text{-}27)$$

where: $w$ is the settlement, $k_{pr}$ is the stiffness of the piled raft foundation and $P$ is the load applied on this foundation.

The stiffness factor for the system is defined by (Randolph, 1994):

$$k_{pr} = \frac{(P_p + P_r)}{w_{pr}} = \frac{[k_p + k_r\,(1 - 2\alpha_{rp})]}{\left[1 - \left(k_r/k_p\right)\alpha^2{}_{rp}\right]} \qquad (2\text{-}28)$$

After point A, the settlement of this foundation can be written as follows:

$$w = \frac{P_1}{k_{pr}} + \frac{(P - P_1)}{k_r} \qquad (2\text{-}29)$$

where, $P$ is the load applied on this foundation, $k_r$ is the stiffness of raft, $P_1$ is the load corresponding to point A (Figure 2-22)

The load settlement curves for a raft with varying pile numbers can be estimated using a computer spreadsheet or a mathematical program such as MATHCAD. The relationship between the number of piles and the average settlement of the foundation may thus be easily calculated. Figure 2-23 depicts the results of a typical set of calculations for both settlement and factor of safety in relation to vertical bearing capacity as a function of pile number. Such calculations provide a quick way to determine if creep piling or full pile capacity utilization design philosophies are likely to be practical.

**(b) Second design stage: assessment of piling requirements**

In the second design stage, assessing piling requirements becomes crucial. While preliminary phases often assume uniformly distributed loading over the raft surface, this oversimplification doesn't account for precise loading patterns, especially when column loadings are involved. To address this, a method is proposed for calculating the maximum column loadings that the raft can support in scenarios where no pile is situated beneath the column.

Figure 2-24 depicts a typical raft column. A pile beneath the column may be deemed necessary in at least four situations:

1. If the maximum moment in the raft below the column surpasses the allowable value for the raft.
2. If the maximum shear in the raft below the column exceeds the allowable value for the raft.
3. If the maximum contact pressure below the raft surpasses the allowable design value for the soil.
4. If the maximum local settlement below the column exceeds the allowable value.

The elastic solutions summarized by Selvadurai (1979) can be used to estimate the maximum moment, shear, contact pressure, and local settlement caused by column loading on the raft. These are for the ideal case of a single concentrated load on a semi-infinite elastic raft supported by a homogeneous elastic layer of great depth, but they do at least provide a rational basis for design.

1) Criteria for maximum moment:

The following approximations produce the maximum moments $M_x$ and $M_y$ below a column of radius $c$ operating on a semi-infinite raft:

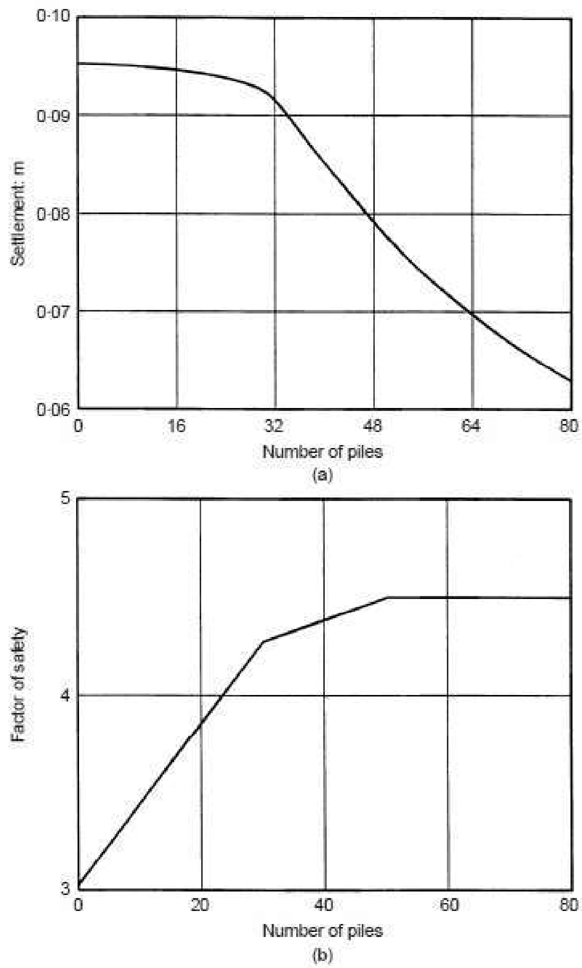


Figure 2-23 : Typical results from MATHCAD analysis: (a) settlement, (b) factor of safety plotted against number of piles (after Poulos, 2001)

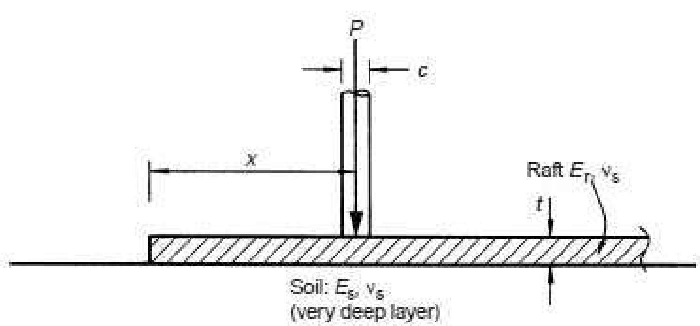


Figure 2-24: Definition of problem for an individual column load (after Poulos, 2001)

$$M_x = A_x P \qquad (2\text{-}30)$$

$$\boldsymbol{M_y = B_y P} \qquad (2\text{-}31)$$

where, $A_x = A - 0.0928\ln(^{c}/_{a})$;$B_y = B - 0.0928\ln(^{c}/_{a})$; $A, B$= coefficients depending on $^{x}/_{a}$; $x$ = distance of the column centre line from the raft edge; $a$ = characteristic length of raft $= t[E_r(1-\nu_s{}^2)/6E_s(1-\nu_r{}^2)]^{1/3}$; $t$= raft thickness; $E_r$ = raft Young's modulus; $E_s$= soil Young's modulus; $\nu_r$= raft Poisson's ratio; and $\nu_s$= soil Poisson's ratio. The coefficients $A$ and $B$ are plotted in Figure 2-25 as a function of the relative distance $^{x}/_{a}$

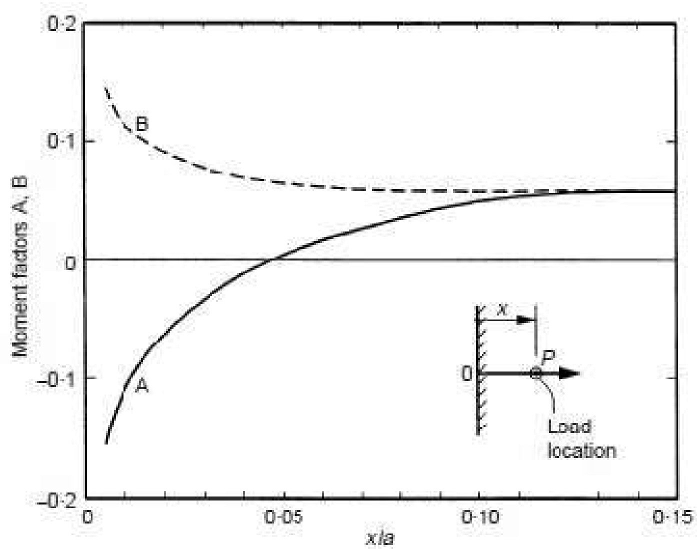


Figure 2-25 : Moment factors A, B for circular column (after Poulos, 2001)

The maximum column load $P_{cl}$ that the raft can carry without exceeding the permissible moment is then given by

$$P_{cl} = \frac{M_d}{larger\ of\ A_x\ and\ B_y} \qquad (2\text{-}32)$$

Where, $\boldsymbol{M_d}$= Design moment capacity of raft

2) Maximum shear criterion.

The maximum shear, $V_{max}$, beneath a column is given as

$$V_{max} = \frac{(P - q\pi c^2)c_q}{2\pi c} \quad (2\text{-}33)$$

Where, $q$ = contact pressure below raft; $c$ = column radius; and $c_q$ = shear factor, plotted in Figure 2-26. As a result, if the raft's design shear capacity is $V_d$, the maximum column load, $P_{c2}$ that can be applied to the raft is

$$P_{c2} = \frac{V_d\, 2\pi c}{c_q} + q_d \pi c^2 \quad (2\text{-}34)$$

Where, $\boldsymbol{q_d}$ = design allowable bearing pressure below raft.

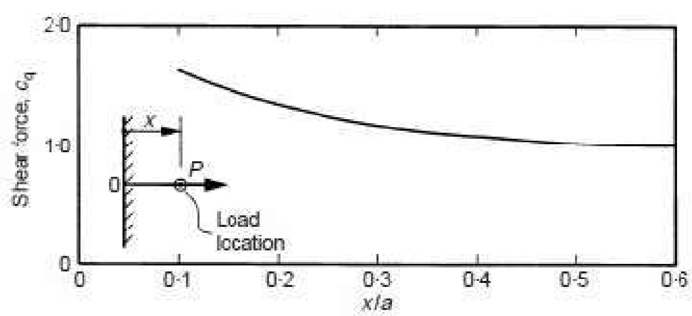


Figure 2-26 : Shear factor, $c_q$ for circular column (after Poulos, 2001)

3) Maximum contact pressure criterion:

The maximum contact pressure at the raft's base $q_{max}$ can be calculated as follows:

$$q_{max} = \frac{P\,\bar{q}}{a^2} \quad (2\text{-}35)$$

Where, $\bar{q}$ = factor is displayed in Figure 2-27 and $a$ = characteristic length is defined in equation (2-30). $P_{c3}$, the maximum column load that can be applied without exceeding the allowed contact pressure, is then calculated.

$$P_{c3} = \frac{q_u a^2}{F_s \bar{q}} \qquad (2\text{-}36)$$

Where, $q_u$ is the ultimate bearing capacity of the soil beneath the raft and $F_s$ is the factor of safety for contact pressure.

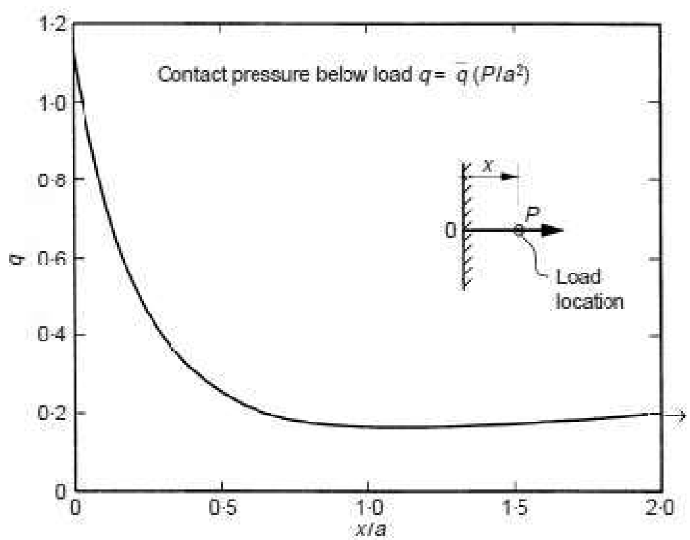


Figure 2-27 : Contact pressure factor, q (after Poulos, 2001)

4) Local settlement criterion

The settlement beneath a column (as a concentrated load) is given by

$$S = \frac{\omega(1 - {\nu_s}^2)P}{E_s a} \qquad (2\text{-}37)$$

where, where $\omega$ = settlement factor is shown in Figure 2-28. This expression does not account for the impacts of adjacent columns on the settlement of the column under consideration, nor does it account for a local settlement superimposed on a more general settlement 'bowl.'

If the permitted local settlement is $S_a$ , then the maximum column load $P_{c4}$ that should not be exceeded is

$$P_{c4} = \frac{E_s\, S_a\, a}{\omega(1 - \nu_s{}^2)} \tag{2-38}$$

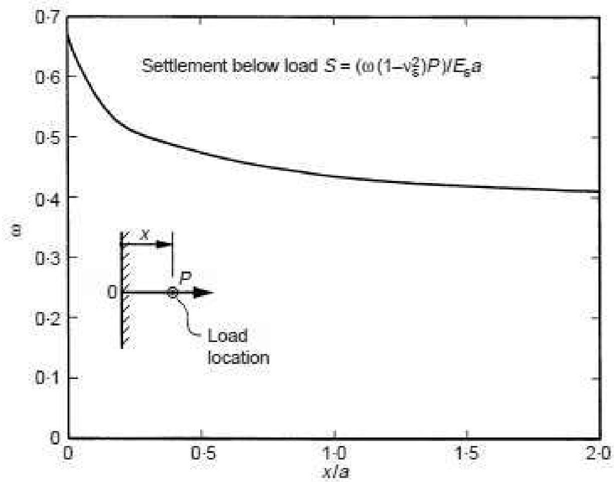


Figure 2-28 : Settlement factor, $\omega$ (soil assumed to be homogeneous and very deep) (after Poulos, 2001)

Assessment of pile requirements for a column location: If the actual design column load at a given point is $P_c$, a pile will be required if Pc exceeds the least of the four criteria listed above. That is, assuming

$$P_c > P_{crit} \tag{2-39}$$

where, $P_{crit}$ is minimum of $P_{c1}, P_{c2}, P_{c3}\ or\ P_{c4}$

If the critical criterion is maximum moment, shear, or contact pressure (i.e. $P_{crit}$ is $P_{c1}, P_{c2}$ or $P_{c3}$), the pile should be constructed to meet the deficiency in load capacity. According to

Burland (1995), only around 90% of the final pile load capacity should be considered mobilized beneath a piled raft system. On this basis, the ultimate pile load capacity,$P_{ud}$ at the column site is calculated as follows:

$$P_{ud} = 1.11\, F_p(P_c - P_{crit}) \tag{2-40}$$

where, $F_p$ is the pile safety factor. While designing piles as settlement reducers, $F_p$ can be assumed to be unity. If local settlement is the important criterion, the pile should be constructed to give adequate extra stiffness. The target stiffness, $K_{cd}$, of the foundation below the column is determined at a maximum local settlement of $S_a$.

$$K_{cd} = \frac{P_c}{S_a} \tag{2-41}$$

Using equation (2-22) as a first approximation, the required pile stiffness, $k_p$ to attain this goal stiffness can be determined by solving the following quadratic equation:

$${k_p}^2 + k_p\left[k_r\left(1 - 2\alpha_{cp}\right) - k_{cd}\right] + {\alpha_{cp}}^2 k_r k_{cd} = 0 \tag{2-42}$$

where, $\alpha_{cp}$ is the raftpile interaction factor and $k_r$ is the raft stiffness around the column. The raft stiffness $k_r$ can be determined as the stiffness of a circular foundation with a radius equal to the characteristic length, $a$ (assuming that this does not result in a total raft area that exceeds the actual area of the raft).

**(c) Detailed design stage:**

Once the preliminary stage has determined that a piled raft foundation is feasible and an indication of the likely piling requirements has been obtained, a more detailed design is required to assess the detailed distribution of settlement and decide on the optimum locations and arrangement of the piles. The raft bending moments and shears, as well as the pile loads, should be obtained for the foundation's structural design.

Poulos et al. (1997) described some of the methods for studying piled rafts that have been developed. The less simplified numerical analysis methods tend to fall into the following categories:

(a) Techniques based on a strip-on-springs approach, in which the raft is represented by a sequence of strip footings and the piles by appropriate stiffness springs (e.g. Poulos, 1991).

(b) Techniques based on a 'plate on springs' approach, in which the raft is represented by a plate and the piles by springs (e.g. Clancy & Randolph, 1993; Poulos, 1994a; Russo & Viggiani, 1998; Yamashita et al., 1998; and poulos & Georgiadis, 1998).

(c) Boundary element approaches, in which both the raft and the piles within the system are discredited and elastic theory is used (e.g., Butterfield & Banerjee, 1971; Kuwabara, 1989; and Sinha, 1997)

(d) Approaches that combine boundary element analysis for piles and finite element analysis for rafts (e.g., Hain & Lee, 1978; Ta & Small, 1996; and Franke et al., 1994).

(e) Simplified finite element analyses, which often involve the foundation system being represented as a planar strain problem (Desai, 1974) or an axi symmetric problem (Hooper, 1974).

**Burland's Approach**

**Burland (1995)** developed the following simplified design approach for piles designed to act as settlement reducers and to achieve their full geotechnical capacity at the design load:

In the absence of piles, determine the total long-term load-settlement relationship for the raft (see Figure 2-29). The design load $P_0$ yields the total settlement $S_0$. Determine an acceptable design settlement $S_d$, including a margin of safety.

Choose a design settlement $S_d$ that is acceptable and includes a safety factor.

$P_1$ is the raft's load, which corresponds to $S_d$.

It was believed that settlement-reducing piles support the extra load $P_0$-$P_1$. No safety factor was used because the shaft resistance of these piles would be fully mobilized. Burland, on the other hand, suggested multiplying the "conservative best estimate" of ultimate shaft capacity, $P_{su}$, by a "mobilization factor" of roughly 0.9.

$$Q_r = Q - 0.9P_{su} \tag{2-43}$$

After that, the bending moments in the raft could be estimated by examining the piled raft as if it were a raft subjected to lower loads, $Q_r$. Burland did not specifically explain the method for predicting the piled raft's settlement, although it looks possible to utilize **Randolph's (1994)** approximate methodology, which states:

$$S_{pr} = S_r \frac{k_r}{k_{pr}} \tag{2-44}$$

where, $S_{pr}$ = settlement of piled raft

$S_r$= settlement of raft without piles subjected to the total applied loading

$k_r$= stiffness of raft

$k_{pr}$ = stiffness of piled raft.

Equation (2-28) can be used to estimate $k_{pr}$.

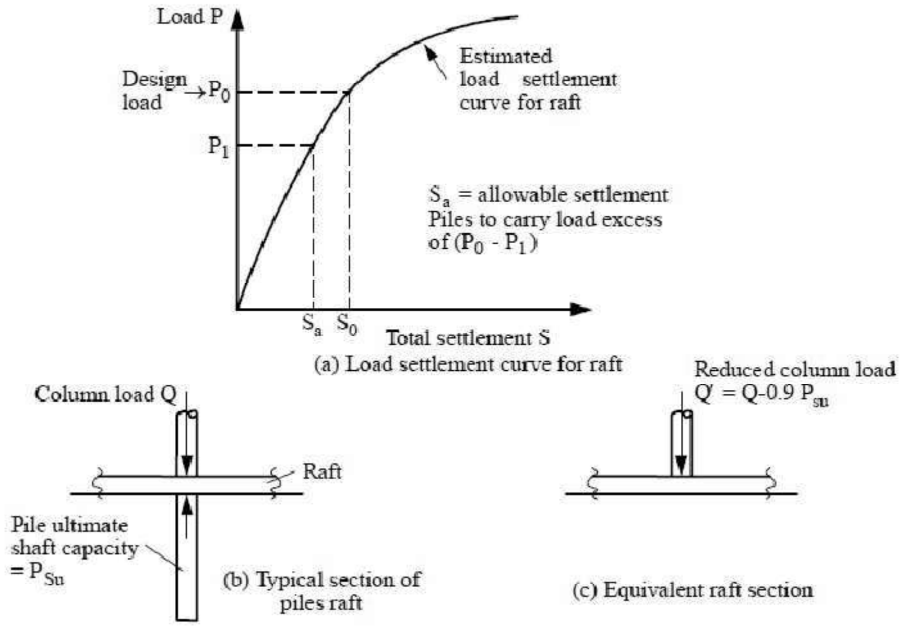


Figure 2-29 : Burland's simplified design concept (after Burland, 1995)

**Omeman et al. (2012)** created a simple model for predicting raft-pile settlement and load sharing for piled-raft foundations. This model can help foundation engineers formulate piled-raft foundations, especially in the early stages of the design process, as well as conduct feasibility studies to assess various alternatives. Engineers can save a lot of time and effort by employing this model instead of a complicated numerical analysis that requires special tools. Because piled-raft foundations are a combination of raft and pile foundations, the stiffness of piled-raft foundations, $k_{pr}$ was considered to be a combination of the stiffness of the raft, $k_r$ and the stiffness of the piles, $k_p$ as provided by the equation (2-45).

$$k_{pr} = k_r + k_p \tag{2-45}$$

As a result, equation (2-45) cannot adequately represent the stiffness of the piled-raft foundations' system. As a result, equation (2-45) had been changed to equation (2-46) to account for the influence of the raft-pile interaction. New factors called raft stiffness and pile stiffness efficiency factors had been proposed in this equation.

$$k_{pr} = \alpha_r k_r + \alpha_p k_p \qquad (2\text{-}46)$$

Equations (2-47) and (2-48) can be used to calculate the load sharing between the raft and the piles:

$$Raft\ load\ \% = 100 * \left(\frac{\alpha_r k_r}{k_{pr}}\right) \qquad (2\text{-}47)$$

$$Pile\ load\ \% = 100 - Raft\ load\ \% \qquad (2\text{-}48)$$

where $\alpha_r$ is the efficiency factor for modifying the stiffness of the raft due to the influence of the pile, and $\alpha_p$ is the efficiency factor for modifying the stiffness of the piles due to the effect of the raft. $k_r$ and $k_p$ can be estimated using standard methods from the literature. The constructed model PLAXIS 2-D was used to determine the value of the interaction factor, $\alpha_r$ and the number of examples of piled-rafts supported by a single pile with varying pile-raft stiffness ratios. For each scenario, the raft load, $k_p$, $k_r$, and $k_{pr}$ were calculated. Then, for each scenario, $\alpha_r$ was computed using equation (2-47). The value of $\alpha_p$ was then calculated by replacing the value of $\alpha_r$ in equation (2-46). As demonstrated in Figure 2-30 and Figure 2-31, the interaction factors $\alpha_r$ and $\alpha_p$ varied with the stiffness ratio of the piles to the raft, $k_p/k_r$. The interaction factors $\alpha_r$ and $\alpha_p$ were estimated graphically using equations (2-49) and (2-50).

The load sharing between the raft and the piles can be determined using the ratio of the raft's load to the piled-raft's load at the same amount of settlement as given by equation (2-47) Equation (2-48) can be used to calculate the load carried by the piles.

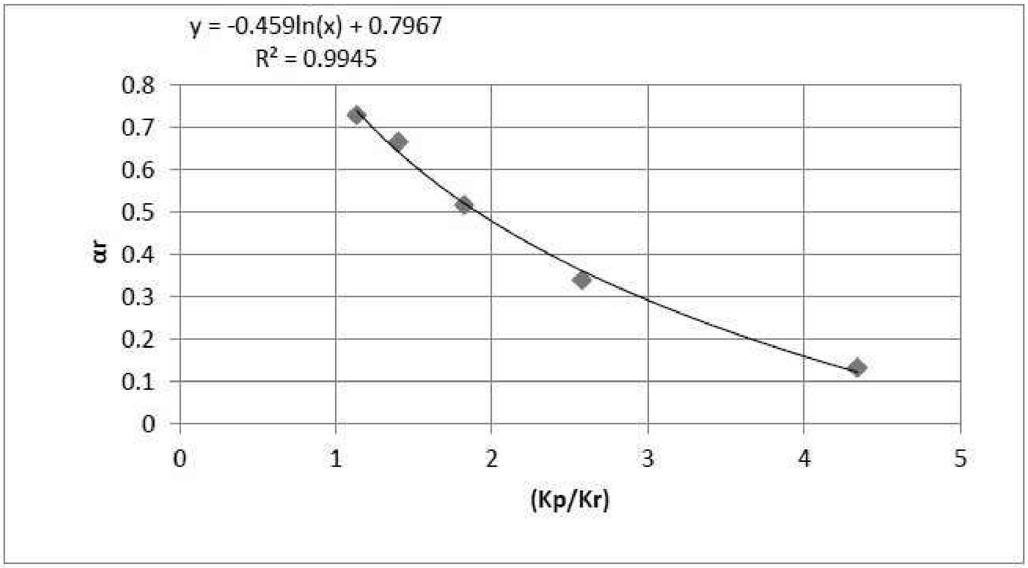


Figure 2-30 : Effect of pile-raft stiffness ratio on the raft efficiency factor, $\alpha_r$, (after Omeman et al., 2012)

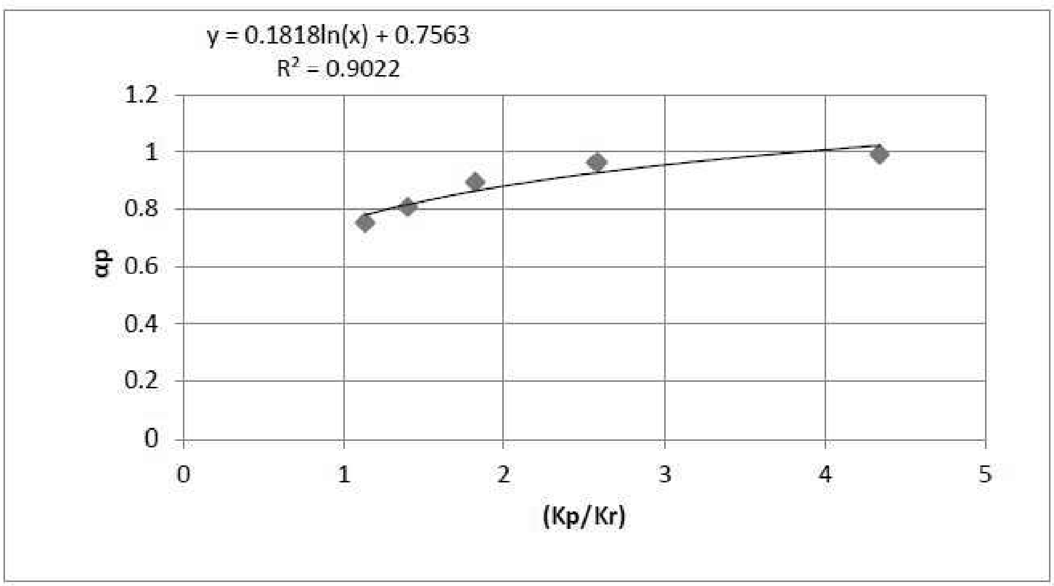


Figure 2-31: Effect of pile-raft stiffness ratio on the pile efficiency factor, $\alpha_p$, (after Omeman et al., 2012)

$$\alpha_r = -0.459 * ln\left({k_p}/{k_r}\right) + 0.7967 \tag{2-49}$$

$$\alpha_p = -0.1818 * ln\left({k_p}/{k_r}\right) + 0.7563 \tag{2-50}$$

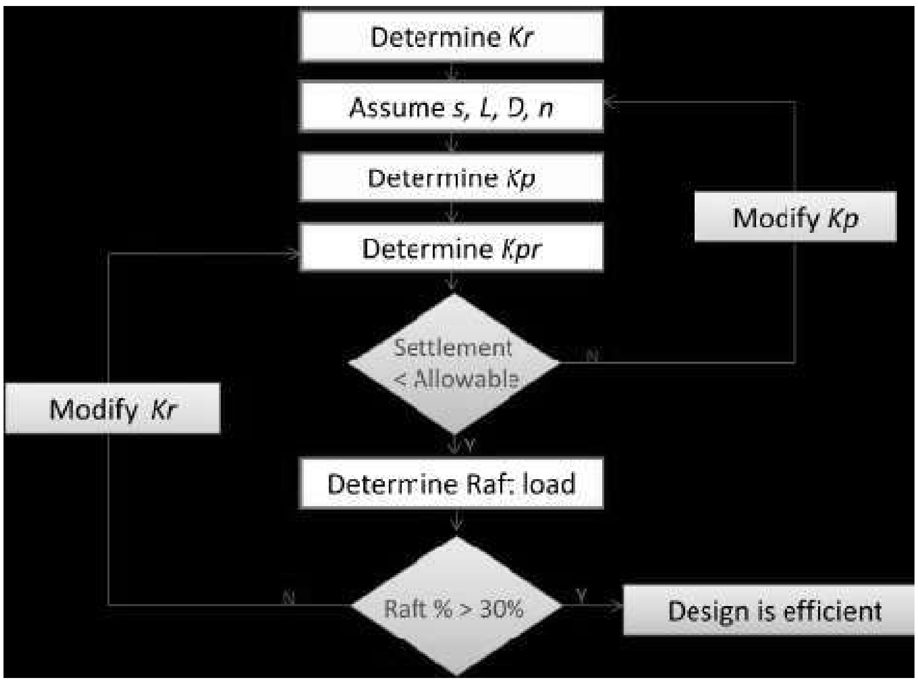


Figure 2-32 : Procedure for preliminary design of piled-raft foundations (after Omeman et al., 2012)

Figure 2-32 depicts a flow chart of this procedure:

1) Calculate the stiffness of the raft foundation alone, $k_r$.

2) To reduce raft settlement, examine a variety of pile groups with varying numbers of piles, pile length, pile diameter, and pile spacing.

3) For each scenario, calculate the stiffness of the pile group without the raft, $k_p$.

4) Determine the settlement of the piled-raft foundations for each scenario using the stiffness of the piled-raft foundations, $k_{pr}$ as given by equation (2-46).

5) If the anticipated settlement exceeds the structure's permissible settlement, change $k_p$ and return to step 2.

6) Using equation (2-47) estimate the load sharing between the piles and the raft for the cases that meet the settlement requirements.

7) If the load shared by raft is less than 30%, change $k_r$ and return to step 4.

8) Repeat the method until the raft's settlement and load criteria are met.

**Lee et al. (2014)** delved into the load response and load carrying capacity of piled rafts, with a focus on the non-linear load sharing behaviour inherent in such systems. They introduced a settlement-based load sharing model for piled rafts, which utilized the normalized non-linear load–settlement relationship while considering the interaction effect between piles and raft. According to their proposed model, the load sharing ratio $\alpha_p$ decreases as settlement increases, with the rate of decrease dependent on the load capacity ratio. Higher load capacity ratios correspond to higher values of $\alpha_p$. The validity of the proposed load sharing model was confirmed through centrifuge load tests, where the calculated values of $\alpha_p$ closely matched the measured values.They proposed the following normalised load-sharing model, taking into account settlement-dependent load-sharing behaviour and load capacity ratio:

$$\alpha_p = \frac{1}{(\beta * \xi) * \left[\dfrac{a_p * \lambda_B + b_p * \left({}^{s}/_{B_r}\right)}{a_r + b_r * \left({}^{s}/_{B_r}\right)}\right] + 1} \tag{2-51}$$

where $\alpha_p$ is the piled raft coefficient, $\beta$ is the load capacity interaction factor, $\xi$ is the load capacity ratio, $a_r$, $b_r$, $a_p$, and $b_p$ are the model parameters, $s$ is the settlement, $B_r$ and $B_p$ are the raft (or cap) width and pile diameter, and $\lambda_B$ is the foundation size ratio = $B_p/B_r$ The model parameters $a_r$, $b_r$, $a_p$, and $b_p$ are 0.02, 0.8, 0.01, and 0.9, respectively, and represent the functional properties of the raft and piles' normalised non-linear load–settlement curves.

Equation (2-51) was developed based on the normalized load–settlement relationships of rafts and piles, where load and settlement were normalized with ultimate load capacity and foundation geometry (i.e., $B_p$ and $B_r$).

Because the ultimate load capacity and foundation geometry represent the local soil condition and foundation characteristics, the normalization process itself reflects the effect of soil and foundation conditions, indicating the model parameters' uniqueness. The uniqueness of the model parameters of the normalized load–settlement relationships for rafts and piles were also demonstrated by Akbas and Kulhawy (2009), and Dithinde et al. (2006). In Equation (2-51), the load capacity ratio ξ denotes the ratio of the raft (or cap) to pile load capacities and is defined as follows Equation (2-52):

$$\xi = \frac{Q_{ult,r}}{Q_{ult,pg}} = \frac{Q_{ult,r}}{\chi_g \sum Q_{ult,sp}} \qquad (2\text{-}52)$$

$Q_{ult,r}$, $Q_{ult,pg}$, and $Q_{ult,sp}$ are the ultimate load capacities of an unpiled raft (or cap), group piles, and a single pile, respectively, and $\chi_g$ is the pile group effect factor. In Equation (2-51), the load capacity interaction factor $\beta$ represents changes in the load-carrying capacities of a raft and piles when combined to form a piled raft due to the pile–raft interaction effect. The pile–raft interaction effect is small in clays, and the value of $\beta$ can be assumed to be 1. (Park and Lee, 2014; and Phung, 1993).

However, the interaction effect is quite large for piled rafts in sands, producing a different load-carrying behaviour than unpiled rafts and group piles (Salgado et al., 1993). For such cases with higher interaction effects, $\beta$ cannot be assumed to be equal to 1, and certain changes to the value of $\boldsymbol{\xi}$ are required (Salgado et al., 1993).

**Alsanabani (2017)** proposed simplified method for computing the load carried by piles, and settlement of piled raft based on the characteristics of an un-piled raft, pile group, and soil. In this study, the stiffness values of the piled raft ($k_{pr}$), unpiled raft ($k_{ur}$), a

3nd pile group ($k_{pg}$) for a certain settlement were used. They used the following relationship for developing the method. The maximum acceptable settlement of a pile foundation is 25 mm, according to ACI-318, whereas the maximum allowable settlement of a pile and raft is 25 mm and 50 mm, respectively, according to ACI-318 and Bowels (1997). The total of the raft and pile loads is the piled raft load, which was stated as follows:

$$Q_{pr} = Q_r + Q_p \tag{2-53}$$

$$\boldsymbol{Q_{pr} = \alpha_{ur} Q_{ur} + \alpha_{pg} Q_{pg}} \tag{2-54}$$

where, $Q_{pr}$ = the total load on piled raft foundation; $Q_r$= the load shared by raft in piled raft foundation; $Q_p$= the load shared by piles in piled raft foundation; $Q_{ur}$ and $Q_{pg}$= loads of the unpiled raft and pile group, respectively which cause a settlement of 25 mm; $\alpha_{ur}$ and $\alpha_{pg}$ = load efficiency factors for the raft and piles, respectively.

Therefore, $\alpha_{ur}$ and $\alpha_{pg}$ represent the ratios of load capacities for the raft and piles that are combined into a piled raft to those of the unpiled raft and pile group ($\alpha_{ur}$ = $Q_r/Q_{ur}$ and $\alpha_{pg}$ = $Q_p/Q_{pg}$). The stiffness is defined as a ratio of the loads to the settlement, the stiffness of the piled raft can be determined using equation given below (Omeman 2012).

$$k_{pr} = \alpha_{ur} k_{ur} + \alpha_{pg} k_{pg} \tag{2-55}$$

where, $\boldsymbol{k_{pr}}$= stiffness of the piled raft; $\boldsymbol{k_{ur}}$= stiffness of the unpiled raft; $\boldsymbol{k_{pg}}$= stiffness of the pile group

Based on stiffness criteria the $\alpha_{ur}$ and $\alpha_{pg}$ can be computed using following equations (Omeman 2012).

$$\alpha_{ur} = (Raft\%) k_{pr}/k_{ur} \tag{2-56}$$

$$\boldsymbol{\alpha_{pg}} = (\boldsymbol{Pile}\%)\boldsymbol{k_{pr}}/\boldsymbol{k_{pg}} \tag{2-57}$$

where "Raft%", and "Pile%" are the percentages of load that are shared by the raft and pile, respectively in piled raft system. Where, $k_{pr}$ is the ratio of the load to the average settlement of the piled raft ($k_{pr} = {Q_{pr}}/{\delta_{ave}}$). The stiffness values of the unpiled raft ($k_{ur}$) and pile group ($k_{pg}$) were calculated using the unpiled raft and pile group models; the stiffness values of the unpiled raft ($k_{ur}$) and pile group ($k_{pg}$) are the load to average settlement ratios of the unpiled raft and pile group, respectively.

Figure 2-33 depicts the relationship between the pile group coefficient and the unpiled raft coefficient $\left({\alpha_{pg}}/{\alpha_{ur}}\right)$ and the ratio of the unpiled raft stiffness to the pile group stiffness $\left({k_{ur}}/{k_{pg}}\right)$ for various sand conditions. These data's correlations ranged from 0.97 to 0.98, which is regarded excellent. According to Figure 2-33, as the ratio stiffness $\left({k_{ur}}/{k_{pg}}\right)$increases, the ratio of efficiencies load factors $\left({\alpha_{pg}}/{\alpha_{ur}}\right)$ decreases. In other words, as the raft stiffness or pile group stiffness increases, the load shared by piles decreases. Equations (2-56) and (2-57) were used initially to calculate "Raft%" and "Pile%." The value of $\left({\alpha_{pg}}/{\alpha_{ur}}\right)$ can be determined from the given value of $\left({k_{ur}}/{k_{pg}}\right)$ using Figure 2-33 and the sand condition. The value of $T$ is calculated as $T = \frac{{\alpha_{pg}}/{\alpha_{ur}}}{{k_{ur}}/{k_{pg}}}$. Finally, Raft% and Pile% can be calculated using equations (2-58) and (2-59).

$$\boldsymbol{Raft}\,\% = \frac{\mathbf{1}}{\mathbf{1}+\boldsymbol{T}} \tag{2-58}$$

$$\boldsymbol{Pile}\ \% = \frac{\boldsymbol{T}}{\boldsymbol{1+T}} \quad (2\text{-}59)$$

They validated the data, which reveal that the load sharing estimated using the simplified technique correlates well with the PDR method for pile spacing values of *3D* and *5D*. However, there were significant variances for the pile spacing value of *7D*. This was related to differential settlement in piled raft models, which rose as pile spacing increased. The raft-soil stiffness ($k_{rs}$) was greater for pile spacing values of *3D* and *5D* than for pile spacing of *7D*.

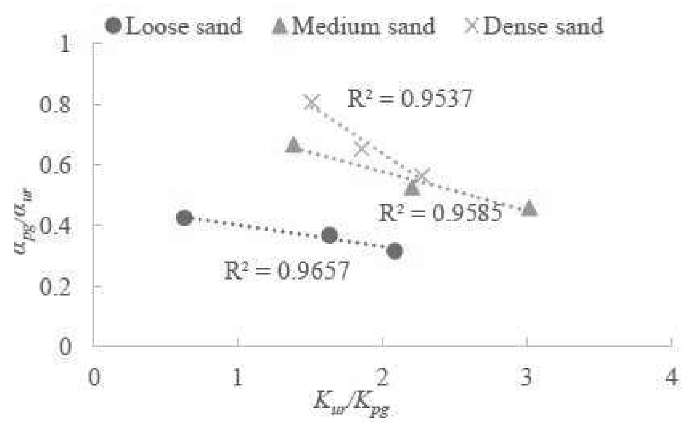


Figure 2-33: $\alpha_{pg}/\alpha_{ur}$ versus $k_{ur}/k_{pg}$ for loose, medium, and dense sand (after Alsanabani, 2017)

**Bhartiya et al. (2020)** performed systematic linear-elastic finite-element analyses on a series of unpiled rafts (rafts without piles), pile groups, and piled rafts with different geometries and pile configurations to determine the stiffness of these rafts, pile groups, and piled rafts. They performed parametric studies in conjunction with regression analysis based on which equations were proposed for quick estimation of piled raft stiffness by combining the stiffness's of unpiled rafts and pile groups. The average and maximum settlements of piled rafts were calculated using the piled raft stiffness equations. They suggested the following flowchart (Figure 2-34) for the estimation of piled raft settlement.

This study's ultimate purpose was to forecast the settlement reaction of a PRF system. They calculated soil subgrade modulus $k_s$ (kN/m$^3$) using equation (2-60) suggested by (Vallabhan et al. 1991; and Turhan, 1992) for a plate-soil system as a result of a rigorous, continuum-based analytical analysis of beams and plates on elastic foundations.

$$k_s = \frac{E_s(1-\mu_s)}{(1+\mu_s)(1-2\mu_s)\sqrt{A_r}} \tag{2-60}$$

where, $A_r$ = plan area of the raft

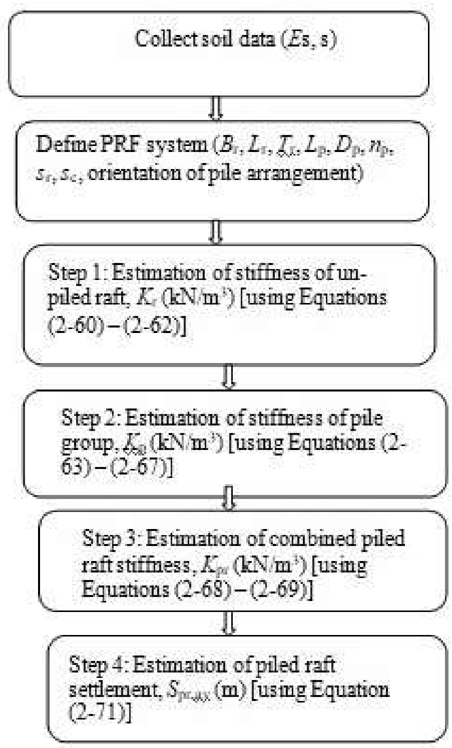


Figure 2-34 : Flowchart for the estimation of piled raft settlement (adapted from Bhartiya et al., 2020)

However, because Vallabhan et al. (1991) and Turhan (1992) made simplified assumptions about the soil displacement field in their analysis of beams and plates, Equation (2-60) did not match with the average stiffness $k_r$ (kN/m$^3$) of rafts, which is analogous to the subgrade modulus and was calculated from the FE analysis of rafts performed in their study. $k_r$ is defined as the applied uniformly distributed load (kN/m$^2$) at the raft's top divided by the average (arithmetic mean) of raft settlements at the centre and corners. Because of the mismatch, a FE-based systematic parametric investigation was carried out to derive a semi empirical equation for $k_r$ by fitting the FE analysis results with carefully selected raft-soil interaction parameters. Keeping the theoretical character of the subgrade modulus given by Equation (2-60) in mind, the raft subgrade modulus was stated as

$$k_r = k_s k_{rs} \tag{2-61}$$

$k_{rs}$ denoted the dimensionless raft-soil interaction factor. Important characteristics influencing the raft response were found in order to define the functional form of $k_{rs}$ (=$k_r/k_s$).

$$k_{rs} = 0.865 C_s \, log_{10}\left(\frac{L_r}{T_r}\right)\left(\frac{1-{\mu_s}^2}{1-{\mu_r}^2}\right)\left[1-\left(\frac{T_r}{B_r}\right)^3\right] e^{-30\left({E_s}/{E_r}\right)} \tag{2-62}$$

where, $\mu_r$ = poisson's ratio of raft; $C_s$= shape factor = $\left({B_r}/{L_r}\right)^{0.25}$ for rectangular or strip rafts, and 0.85 for circular rafts

Pile Group Stiffness

They calculated the individual pile stiffness $k_{p1}$ (which includes both the structural and geotechnical components of stiffness) using three-dimensional FE analysis of single piles with varying diameters ($D_p$ = 0.5-1.5 m) and lengths ($L_p$ =10-20 m) for the different soil types and derived the following equation for stiffness of single pile

$$k_{p1} = I_{ps} A_p E_p / L_p \tag{2-63}$$

where, $k_{p1}$= individual pile stiffness; $I_{ps}$= dimensionless influence factor which considered the effect of the pile–soil interaction; $A_p$= cross-sectional area of pile; $E_p$= Young's modulus of pile; $L_p$= length of pile

$$I_{ps} = 0.0084\left(\frac{\mu_p}{\mu_s}\right)\left(\frac{L_p}{D_p}\right)e^{-0.001\left(\left(E_p/E_s\right)\left(L_p/D_p\right)\right)^{0.034}} \tag{2-64}$$

$\mu_p$= poisson's ratio of pile; $\mu_s$= poisson's ratio of soil; $D_p$= diameter of pile; $E_s$= Young's modulus of soil

In order to consider the combined effect of these parameters on the pile group–soil interaction, a dimensionless parameter $\eta$ was introduced that correlates pile spacing, pile diameter, and the influence area of the pile group to the pile group stiffness

$$\eta = 1 - 0.4\,log_{10}\left(1 - \frac{A_{gp}}{A_r} - \frac{D_p}{2s_r}\right) \text{ for Rectangular or strip PRFs} \tag{2-65}$$

$$\eta = 1 - 0.4\,log_{10}\left(1 - \frac{A_{gp}}{A_r} - \frac{D_p}{s_r}\right) \text{ for Circular PRFs} \tag{2-66}$$

where, $A_{gp}$= cross sectional area of the piles in group taken together; $s_r$= pile spacing along the raft length and width

Based on the observation from FE analysis, they performed regression analysis and proposed following equation for calculating stiffness of pile group

$$k_p = k_{p1}n_p(e^{\eta} - 2)/A_{gp} \tag{2-67}$$

Piled Raft Stiffness

The values of $k_{pr}$ derived using the Randolph (1994) equation and those acquired directly from FE analysis were contrasted. Through trial and error, they modified $k_{pr}$ equation as equation (2-68) - (2-69) to achieve the desired result, which reduced the discrepancy in the results.

$$k_{pr} = \frac{0.38 k_p e^{2.4\left(A_{gp}/A_r\right)} + k_r(1-2\alpha_{pr})}{1+\alpha_{pr}{}^2 k_r/k_p} \text{ for rectangular or strip PRFs} \quad (2\text{-}68)$$

$$k_{pr} = \frac{0.38 k_p e^{2.4\left(A_{gp}/A_r\right)} + k_r(1+2\alpha_{pr})}{1+\alpha_{pr}{}^2 k_r/k_p} \text{ for circular PRFs} \quad (2\text{-}69)$$

Load Sharing in PRF

They discovered from FE analysis that load sharing depends more on the relative stiffness of the raft and piles than it did on the percentage of raft and pile regions through which the loads are passed. Based on several trials and errors and corresponding regression analyses, the following equation of $N_p$ was established, taking into account these facts and noting that the factor $\alpha_{pr}$ takes into account the raft-pile interaction (Randolph, 1994).

$$N_p = \frac{P_p}{P} = \frac{k_p + (1 - 2\alpha_{pr})k_r}{k_p + k_r} \quad (2\text{-}70)$$

where, $P_p$ = load shared by the piles; and $P$ = total applied super structure load.

Estimation of Elastic Settlement of PRF

The stiffness equations derived in the preceding section was utilized to calculate the PRF settlement. The assessment of PRF settlement consists of four major steps: (1) estimation of unpiled raft stiffness $k_r$; (2) estimation of pile group stiffness $k_p$; (3) estimation of PRF stiffness $k_{pr}$; and (4) estimation of average PRF settlement $S_{pr,av}$ using equation (2-71)

$$S_{pr,av} = \frac{\left(P/A_r\right)}{k_{pr}} \quad (2\text{-}71)$$

The elements of the piled-raft foundation are modeled as a plane-strain or axially symmetric problem using a 2-dimensional (2D) numerical analysis. While 2D numerical models are more widely used in the literature, 3D modeling is the recommended approach for studying piled-raft foundations, as briefly discussed below.

**2) Approximate computer–based method:**

Among the various analytical approaches for studying piled raft behaviour, 3D finite element and finite difference analyses offer the highest level of accuracy and complexity. Numerous research based on 3D numerical analysis could be identified in the literature and a few of them that are relevant to the topic of this study are emphasized below.

**Prakaso and Kulhawy (2001)** used simplified linear elastic and nonlinear (elastic plastic) 2-D plane strain finite element models to predict the behaviour of piled raft foundations and proposed a displacement based design procedure for piled raft based on the analysis. They used PLAXIS (software based on finite element method) in their study and claimed that a 2-D plane strain analysis may produce adequate findings for analyzing the piled raft system without excessive time for modeling and computing. The numerical results revealed that the ratios of a pile group to raft width, and pile depth are the most influential elements.

**Poulos (2001)** contrasted the outcomes of plane-strain analyses with those attained from PDR and 3D analysis. The conclusion reached was that the implicit assumption of plane-strain in 2D analysis causes settlements to be over predicted.

**Oh et al. (2008)** used the PLAXIS software to do a complete 3D analysis on a piled raft foundation in sand. The soil profile and soil parameters were remained constant throughout the numerical investigation and a comprehensive parametric study was conducted by altering pile spacing, pile number, pile diameter, raft dimension ratio, and raft thickness. The study's findings revealed that the maximum settlement of piled rafts is influenced by pile spacing and pile number and is independent of raft thickness. The differential settlement of piled rafts, on the other hand, reduces as raft thickness increases.

**Omeman (2012)** used a series of 2D finite element analyses to investigate the effect of different parameters on the load sharing of a piled raft foundation in sandy soil. Figure 2-35 depicts five potential pile group layouts that were investigated. The numerical findings demonstrated that increasing the pile diameter and the number of piles decreases the raft share (Figure 2-36), however, pile length has no effect on piled raft load sharing (Figure 2-37).

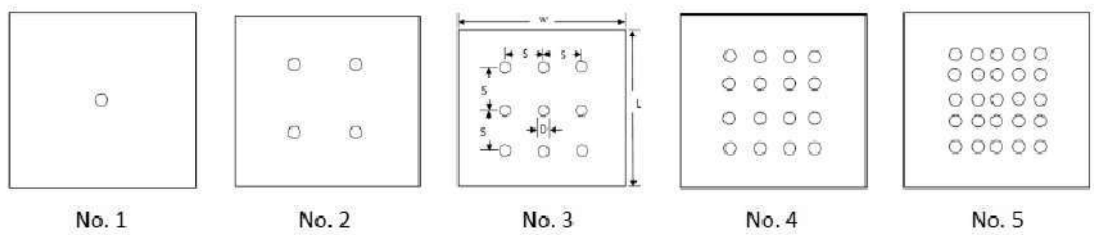


Figure 2-35 : The considered pile raft configuration in 2D analyses (after Omeman, 2012)

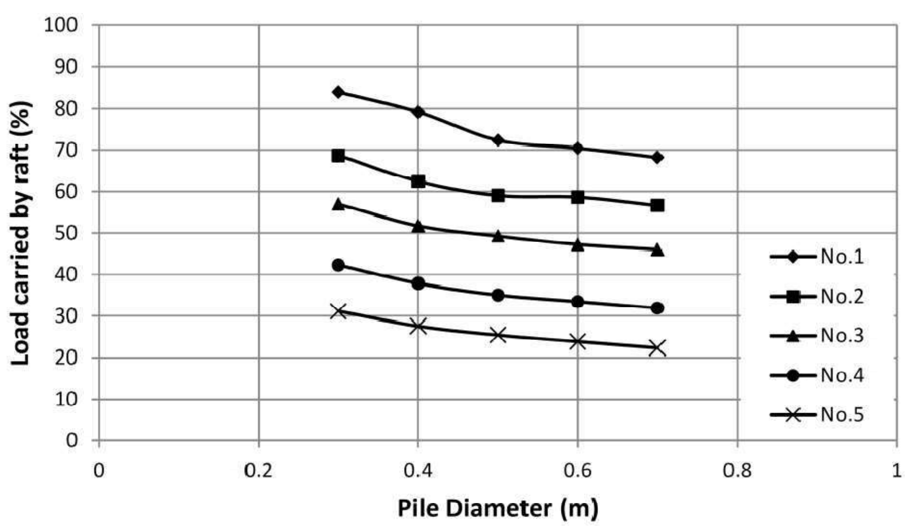


Figure 2-36: Variation of raft share versus pile diameter at a constant load for 5 different piled raft configurations (after Omeman, 2012)

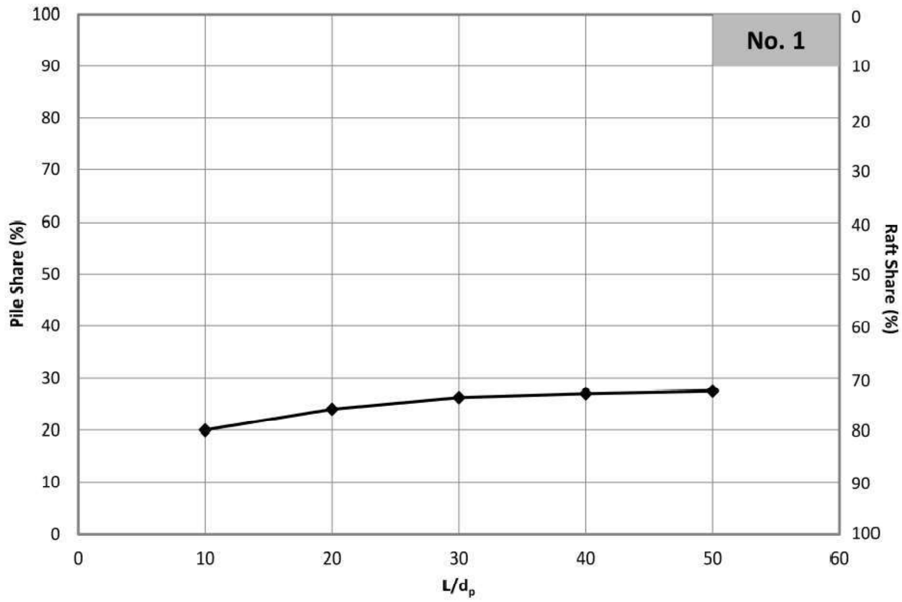


Figure 2-37 : The load sharing of single piled raft unit at 600kPa in different slenderness ratio (after Omeman, 2012)

**Bisht and Singh (2012)** carried out a numerical analysis by using PLAXIS 2-D, to investigate the effect of the above various factors. The aim is to optimally utilize the load-carrying capacity of both the raft and the pile group.

**Sinha (2013)** carried out a number of 3D numerical analyses on a non-displacement piled raft foundation. This numerical study investigated the effect of various parameters on the settlement, bearing capacity, and load sharing of piled rafts. To examine the influence of pile spacing on the load-sharing mechanism, the length over diameter ratio ($L/d_p = 15$) was held constant while pile spacing varied from $2d_p$ to $7d_p$. Table 2-3 has more information regarding the geometry of piled rafts. Figure 2-38 depicts the influence of pile spacing on the load-settlement curve, and it can be shown that increasing the pile spacing increases the settlement of the piled raft. Based on this observation, Sinha (2013) advised against utilizing piled raft with pile spacing more than $6d_p$.

Table 2-3 the geometrical information of piled raft models and the recorded load sharing at 0.5MPa

| Pile Spacing | Raft Size $(B_r \times L_r \times t_r)$ | No. of Piles | Length of Pile (m) | Pile Diameter (m) | Applied Load (MPa) | Load Share (%) | |
|---|---|---|---|---|---|---|---|
| | | | | | | Raft | Pile |
| 2D | 24x24x2m | 144 | 15 | 1 | 0.5 | 14 | 86 |
| 3D | 24x24x2m | 64 | 15 | 1 | 0.5 | 15 | 85 |
| 4D | 24x24x2m | 36 | 15 | 1 | 0.5 | 37 | 63 |
| 6D | 24x24x2m | 16 | 15 | 1 | 0.5 | 66 | 34 |
| 7D | 28x28x2m | 16 | 15 | 1 | 0.5 | 67 | 33 |

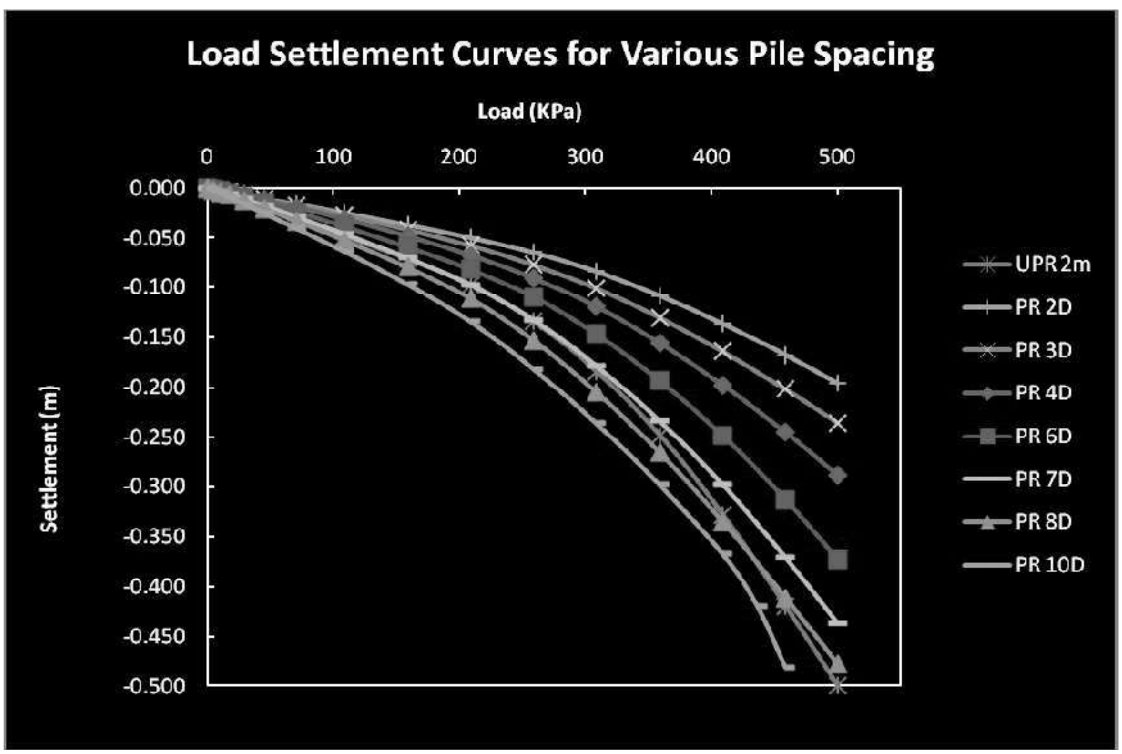


Figure 2-38 : Influence of pile spacing on load settlement behaviour (after Sinha, 2013)

Figure 2-39 depicts the relationship between load sharing and pile spacing. The figure below shows that when the pile spacing is smaller than $3d_p$, the piles carry 90% of the imposed load.

Furthermore, for spacing between piles greater than $3d_p$, the raft share grows until it approaches saturation (70%) at $S/d_p=6$.

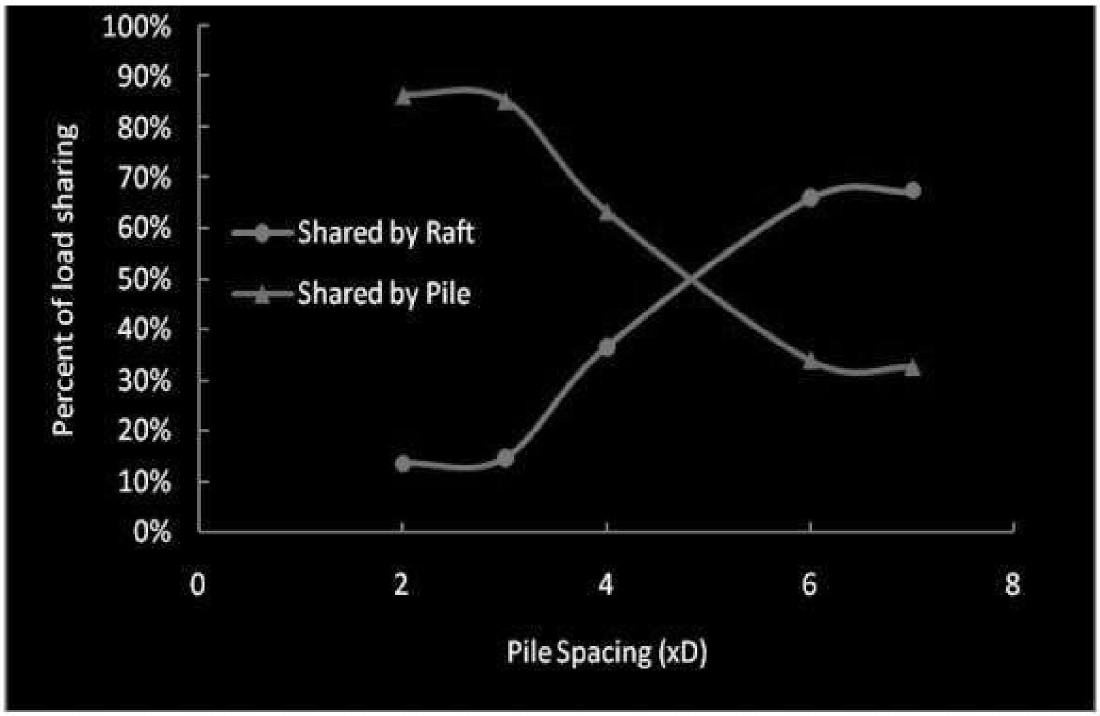


Figure 2-39 : Variation of load sharing versus pile spacing (after Sinha, 2013)

**Bhowmik (2013)** carried out 3D-Finite Element Analysis of piled-raft foundation under vertical load in stone column improved soft clay (Figure 2-40) and concluded that improving soft clay by stone column reduces the total settlement and maximum bending moment of the raft in piled-raft. The axial forces in pile are also reduced due to better raft-soil interaction. He also found that the proportion of total load shared by raft increases with increasing area replacement ratio and slenderness ratio of stone column under piled-raft.

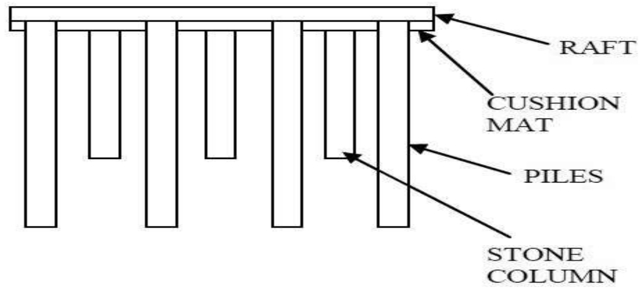


Figure 2-40 : Sketch of Composite Piled Raft System (after Bhowmik , 2013)

**Neto et al. (2014)** used the finite element approach to model four published case histories. In this work, the soil was assumed to be elastic, and the effect of various parameters such as $S/d_p$, $L/d_p$, and stiffness ratio on piled raft behaviour was investigated using numerical analyses. The relative spacing ($S/d_p$) was shown to have a substantial effect on load distribution between the raft and the piles. Furthermore, for a pile spacing of $3d_p$, the foundation serves as a collection of piles that absorbs 94 to 98% of the total applied load. The amount of load borne by the piles reduces as the pile spacing ratio increases.

**Lv et al. (2014)** investigated the influence of pile cross sectional form on the load sharing mechanism of a piled raft foundation. The performance of piled rafts with X-section cast-in-place concrete piles (XCC) was compared to standard circular CCC piled rafts. For the applied load on identical piled raft systems in the study, it was proved that XCC piles bear greater loads than circular piles (66% against 46%). The increased side resistance of XCC piles is the reason of this load sharing difference.

**Adel et al. (2014)** have carried out nonlinear 3D finite difference analysis to model the piled raft problems using the commercial software FLAC3D. They checked the validity of the proposed numerical modeling by a back-analysis was made for a case study. They performed comprehensive parametric study on a hypothetical square piled raft over three clay soil profiles with different degrees of stiffness. The variation had been made in number of piles, length of piles and distribution of piles over the raft area (Figure 2-41). The effect of these variables upon the average settlement and differential settlement had been studied. They concluded that 3D finite difference modeling of piled raft foundation was proved to be efficient for analyzing real piled raft systems.

They also found that the effect of increasing number of piles on differential and average settlement was small but increasing the length of piles had significant effect on that. For softer soil the effect of increasing number of piles became less significant while increasing length of piles became more significant. For the same number of piles, the change in piles' distribution over the raft area has a slight effect on the piled raft average settlement while it has a considerable effect on the piled raft differential settlement.

They have compared the piled raft coefficient $\alpha_{pr}$ calculated by finite difference analysis (0.79) with the value obtained by Reul and Randolph using finite element analysis which is equal to 0.76. Also, the value of the coefficient $\alpha_{pr}$ calculated by Hemaida using finite element analysis was equal to 0.7.

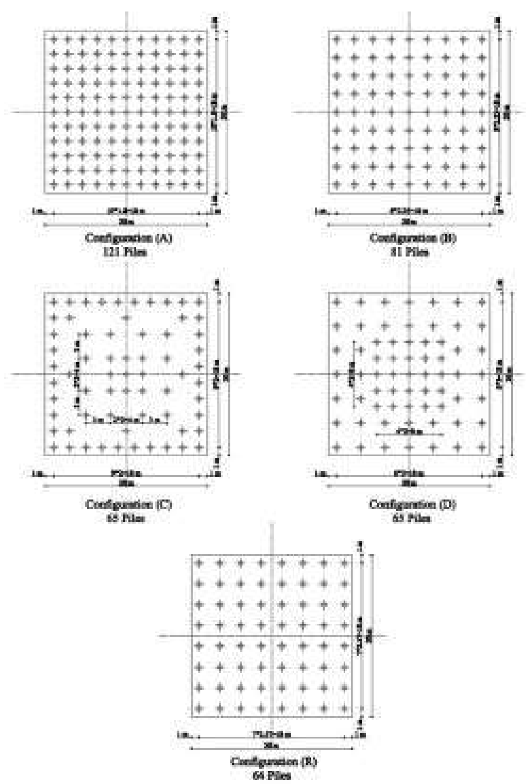


Figure 2-41 : Various Configuration of piled raft foundation (after Adel et al., 2014)

**Wulandari et al. (2015)** carried out a numerical analysis using PLAXIS 2D with the aim to study the settlements of the raft and the piled raft under the same loading. As per the result he found that the addition of piles could reduce the settlement but after words a certain number of piles increasing the number of piles shows the settlement tend to be constant.

**Naveen kumar (2015)** analyzed the piled-raft foundation using ANSYS (2D analysis). They studied the load displacement response of piled raft in a sand medium at various relative densities (loose, medium dense and dense) with interaction effects. Three different pile spacing - 3d, 4d and 5d were considered for the study (where d is the pile diameter) with three different pile configuration (3 × 3, 4 × 4 and 5 × 5) with an objective of finding the optimum number of piles and pile spacing for various relative densities of sand. They observed that the ultimate load and settlement corresponding to ultimate load increases with increase in the relative density. The rate of settlement decreases with the increase in relative density of the soil. The load settlement response of medium and dense sand was found almost identical. The performance of a 4 × 4 pile group was observed to be optimum.

**Chong Yi Hong, Lee et al. (2021)** made parametric study aims to provide insights into the performance of the piled raft foundations subjected to concentrated loading in clay. A series of 2D finite element analyses were performed to investigate the influencing parameters affecting the load distribution and settlement behaviour of the piled raft. The results suggested that increases in both pile length and raft thickness, as well as a decrease in pile spacing would reduce the differential settlement of the piled raft. Comparatively, raft thickness was the most significant controlling parameter affecting the differential settlement. The study also revealed the importance of placing the pile nearer to the location of concentrated load as it would yield a more uniform load distribution, and hence a lower differential settlement.

**Niraula and Acharya (2021)** dealt with successive analysis of parameters of piled-raft foundation system using PLAXIS 2D as a FEM tool. Plain strain analysis of piled raft foundation system had been conducted out by successive fixing up of parameters. For the analysis two cases had been studied for piled-raft lying on silty soil deposit and on clayey deposit with respect to uniform static loading from superstructure. The result of successive variation of parameters showed that variation has limiting effect on load and displacement behaviour.

## 2.4 Case Studies

Some super tall structures have been built on piled raft foundations on non-cohesive soils in the last decade. Most of these constructions, however, are not monitored for settlement and load sharing between piles and raft (Katzenbach et al. 2000, and Yamashita and Yamada 2007). There are just a few real-world case studies that explore the behaviour of piled raft foundations of high-rise buildings in sand. These cases, as described by El-Mossallamy et al. (2006) and Yamashita et al. (2011), are discussed briefly below.

Rolf Katzenbach, et al. (2005) had given an overview of the theoretical and practical development of CPRF foundations and concluded that by using CPRFs as a foundation for high-rise buildings in the settlement-sensitive Frankfurt clay, a considerable settlement reduction of more than 50% compared to raft foundations could be achieved. Due to its enhanced design philosophy, a CPRF reduces the costs for piles by more than 60 % compared to a conventional pile foundation.

### 2.4.1 Multi story building

**Sonoda et al. (2009)** constructed a multi story building and its foundation in sandy ground using a reverse construction method and examined settlements of the foundation for the validity of the design methods. The measured settlements were smaller than those predicted in the design stage, satisfying the design requirements for the building. The main difference between a reverse construction method and a conventional construction method is that the piles are cast in place and are partially loaded by the superstructure early during the construction process. It is only later that the raft (mat foundation) is constructed to combine with the piles to bear the full building load. Therefore, the foundation is regarded as a pile group in early stages of construction, while the foundation behaves as a piled raft after completion of the raft construction. A simple conservative design approach was used for the design of the foundation. To examine the validity of the design method, settlements of the foundation were observed during construction. The measured settlements were smaller than those predicted in the design stage, satisfying the design requirements for the building. Post-analysis of the deformation of the foundation was carried out using the results of the pile load test at the construction site, and the results of the analysis were compared with the observed settlements of the foundation, aiming at an improvement in pile foundation design.

### 2.4.2 Nineteen story residential tower

This project's geotechnical analysis indicated a loose to medium sand layer up to 63 m in depth resting on top of another layer of medium to dense sand (Figure 2-42). It was also discovered that the water level is 3 meters below the ground surface. To prevent overall and differential settlement, a piled raft foundation was proposed for this project. For this project, 28 cast-in-place concrete piles with lengths of 63m, shaft diameters of 1.2 to 1.3m, and toe diameters of 1.8 to 2.2 m were built. A liquefiable silty-sand layer of 10 m thick was discovered at a depth of 8 m. The soil in the depth of 8-18 m was enhanced by grid-form soil cement walls to minimize the substantial shear deformation of the foundation caused by the existence of a liquefiable layer. The recorded measurement on pile P1 revealed that the pile toe load to pile head load ratio was 0.42 both at the end of construction and 15 months later. At the end of construction, the ratio of load borne by the piles to the net load on the tributary area was 0.63 for pile *P1* and 0.66 for pile *P2* (Figure 2-42). After 15 months of pile *P1* and *P2* construction, these ratios increased to 0.69 and 0.77, respectively.

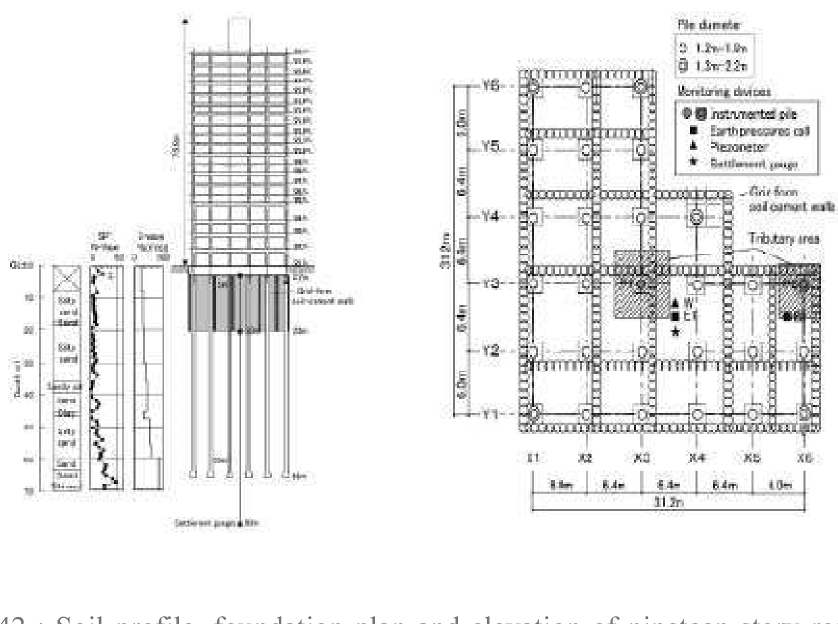


Figure 2-42 : Soil profile, foundation plan and elevation of nineteen story residential tower (after Yamashita et al., 2011)

### 2.4.3 Eleven story office building

The eleven storey office building's elevation and foundation plan, as well as the underlying soil profile, are shown in Figure 2-43. For this project, a piled raft foundation technique was used to regulate the differential settlement. The pile toes of the raft were entrenched in the thick layer of sand and gravel, which was founded on loose sand with SPT-N values of about 10. For this project, cast-in-place concrete piles with 1.1 to 1.5 m shaft diameter are used. The pile measures 27.5 meters in length and has a toe diameter of 1.4 to 1.8 meters. At the end of construction, the ratio of pile toe load to pile head load was 0.25; 32 months later, it had slightly decreased to 0.2. At the end of construction and the most recent observation (32 months after construction), the ratio of the load borne by the piles to the total applied load was 0.54 and 0.65, respectively.

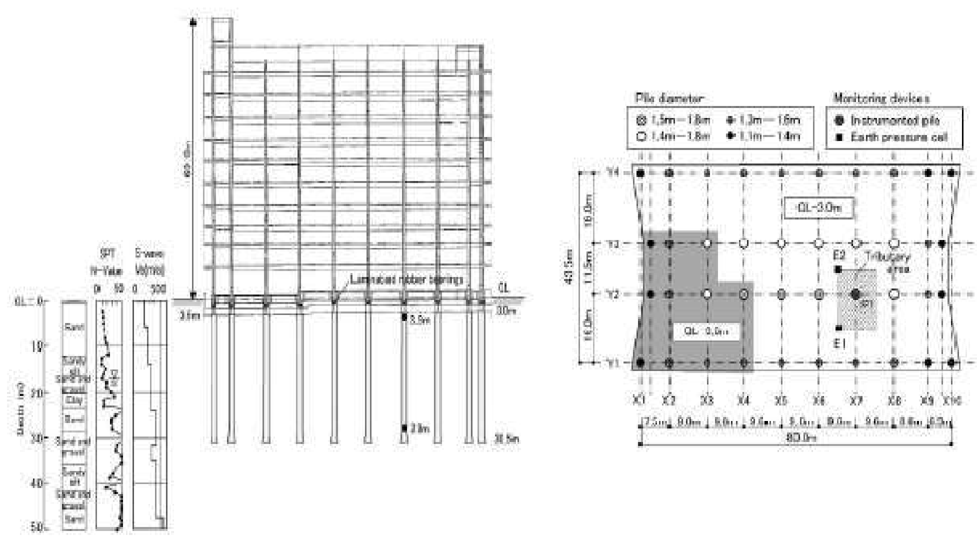


Figure 2-43 : Soil profile, foundation plan and elevation of eleven story base-isolated office building (after Yamashita et al., 2011)

### 2.4.4 Hadron experimental hall

Figure 2-44 shows the foundation layout, height of the foundation, and soil profile beneath the foundation. In the middle of the structure, the raft was supported by dense sand and gravel, and it rested on medium-to-dense sand on the sides. The mat foundation could not offer the permissible settlement due to the existence of a deep saturated cohesive layer at a depth of 23 meters, hence the piled raft foundation was recommended for this project. In this project, 371 drilled pre-cast concrete piles measuring 0.6-0.8 m in diameter and 22-25.7 m in length were employed. The load shared by the piles to the net load ratio for piles *P1* and *P2* was 0.86 and 0.67, respectively, two years after the construction.

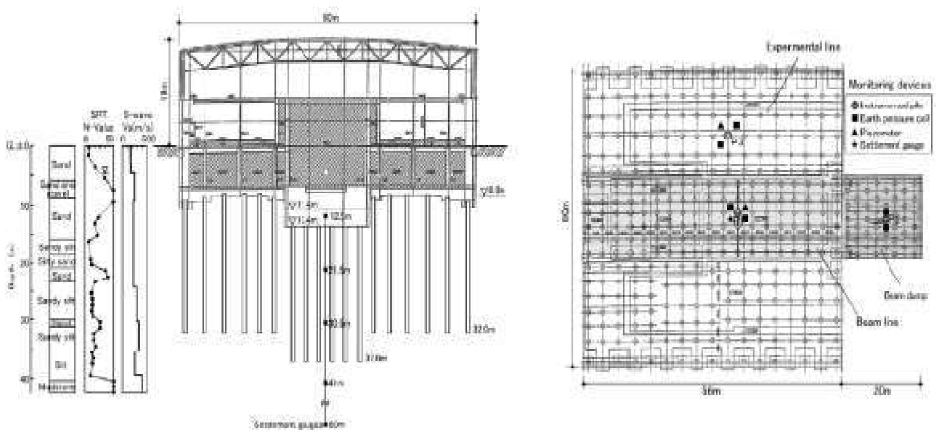

Figure 2-44 : Soil profile, foundation plan and elevation of Hardon experimental hall (after Yamashita et al., 2011)

### 2.4.5 Forty seven story residential tower

Figure 2-45 displays the soil profile and foundation plan for the 47-story residential structure. The pile group, which was made up of 50 m-long cast-in-place concrete piles, was implanted in very dense sand and gravel, while the raft was based in 4.3m of depth on medium sand and gravel. To track how the load was distributed both during and after construction, two piles, *5D* and *7D*, were instrumented with LVDT and strain gauges. The initial values of displacement were noted at the reference point (70 m deep) prior to casting the foundation slab. Then, relative to the reference point, the variation of vertical displacement over time was observed at various depths (Figure 2-46). According to Yamashita et al. (2010), the measured displacement at 5.3 meters of depth is about equivalent to foundation settlement. Eight months after construction was completed, the pile shares for piles *5D* and *7D* were reported to be 0.93 and 0.87, respectively.

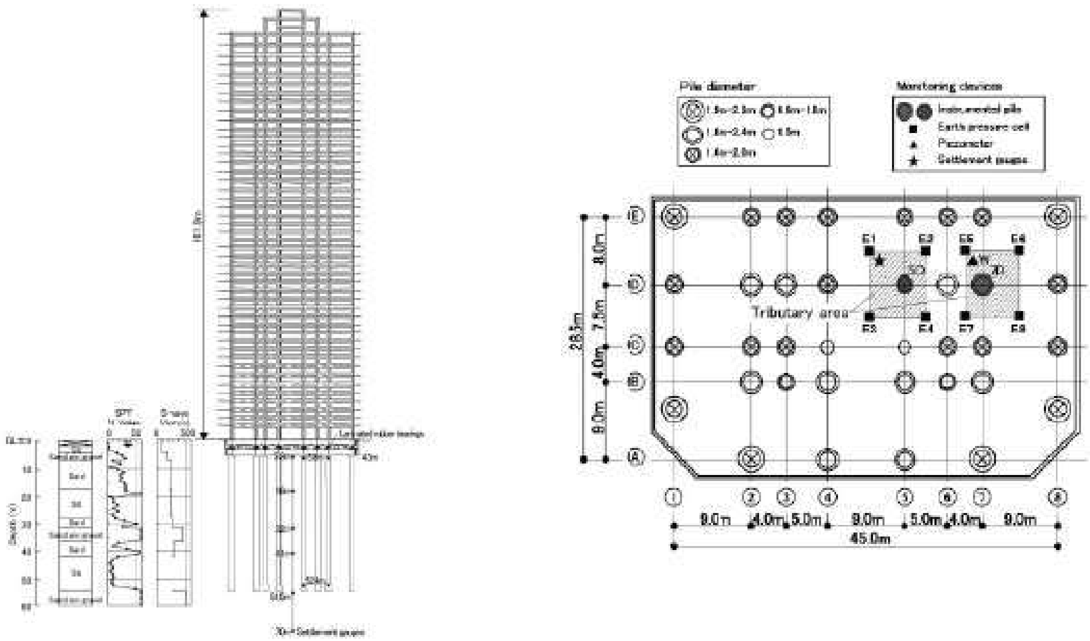


Figure 2-45 : The soil profile and the foundation plan of 47 story residential tower (after Yamashita et al., 2010)

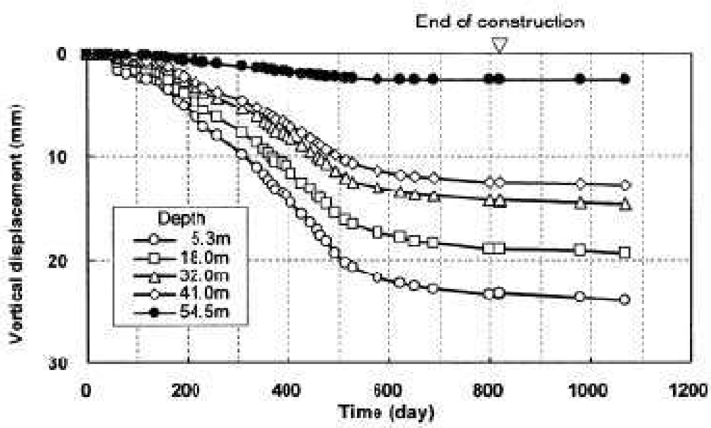


Figure 2-46 : Variation of vertical displacement versus time (after Yamashita et al., 2010)

**Yamashita et al. (2011)** plotted the fluctuation in pile share vs. the average spacing between the instrumented pile and the adjacent piles using the previously reported field measurements (Figure 2-47). This analysis showed that the load shared by piles as a percentage of the net load generally declines as pile spacing increases and nearly remains constant for *S/dp* values over six.

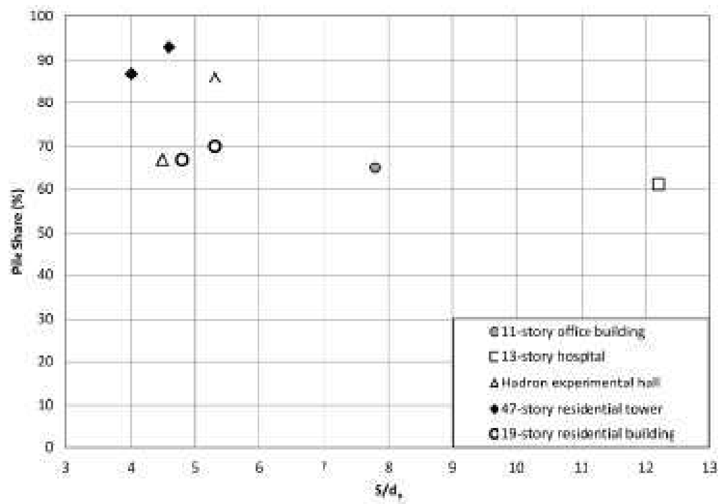


Figure 2-47 : Variation of pile share versus pile spacing in piled raft foundation (after Yamashita et al., 2011)

### 2.4.6 Building tower foundations were designed as pile foundations and found as combined piled raft foundations

It should also be mentioned that some foundations were built as pile foundations, but they functioned as a combined piled-raft foundation, with the raft-bearing portion of the building load. In truth, the distinction between a piled raft and a normal pile foundation is not always clear. If the number of piles is small enough, frictional pile foundations will behave like piled raft.

The PETRONAS Twin Towers in Kuala Lumpur, Malaysia, are an excellent example. The foundation was planned as a standard pile foundation. The raft did, however, carry a portion of the whole load. The raft took 15% of the dead load when the structure reached a height of 34 stories, according to the measurement.

Another example is the ICC Tower in Hong Kong. The foundation was also intended to be a traditional pile foundation. However, the Author claimed in his independent peer-review that the raft could carry a significant portion of the overall load, up to 30%, Phung (2002).

The regulations in Vietnam do not yet accept piled raft foundations. **Trinh et al. (2013)** performed load sharing monitoring on piles and rafts for a modest structure in Hanoi. The building comprises ten floors and a basement floor, with a plan area of approximately 550 $m^2$. At a depth of around 20 m, concrete jacked-down piles with a 30 cm × 30 cm square cross-section were erected in fine to moderately dense sand. Under the columns, piles are set in groups. The pile distance in each group is 90 – 120 cm, or 3 – 4 times the pile width. The foundation is constructed as conventional piles, which carry the entire superstructure weight and have a safety factor of 2.5 to 3.0. Only during the construction stage was monitoring carried out. The axial loads at the pile top, contact pressure under the basement slab, and building settlement were all measured. The measurement revealed a very minor settlement of 7 to 8 mm, which is typical for standard piles. At the end, the piles received up to 77% of the total load, while the raft received 23%. With such a low settlement, the percentage of load carried by the raft in this example appears excessive when compared to the case histories listed in Table 2-4. This can be explained by the building's low-rise design or by the heave of the excavation bottom.

Table 2-4 Piled raft and conventional piled foundations for high-rise buildings - Case Histories (Phung, 2011)

| No | Tower | Structure | | Load share (%) | | Measurement | Settlement |
|---|---|---|---|---|---|---|---|
| | | Height, m | Stories | Piles | Raft | | $s_{max}$ (mm) |
| 1 | Messe-Torhaus, Frankfurt | 130 | 30 | 75 | 25 | Yes | 120 |
| 2 | Messeturn, Frankfurt | 256 | 60 | 57 | 43 | Yes | 144 |
| 3 | Westend 1, Frankfurt | 208 | 53 | 49 | 51 | Yes | 120 |
| 4 | Petronas, Kuala Lampur CPF) | 450 | 88 | 85 | 15 | Yes | 40 |
| 5 | QV1, Perth, West Australia | 163 | 42 | 70 | 30 | N.A. | 40 |
| 6 | Treptower, Berlin | 121 | | 55 | 45 | Yes | 73 |
| 7 | Sony Center, Berlin | 103 | | N.A. | N.A. | Yes | 30 |
| 8 | ICC, Hong Kong CPF) | 490 | 118 | 70 cal) | 30 ca.) | N.A. | 40 cal) |
| 9 | Commerzbank, Frankfurt CPF) | 300 | 56 | 96 | 4 | Yes | 19 |
| 10 | Skyper, Frankfurt | 153 | 38 | 63 | 27 | Yes | 55 |
| 11 | Dubai Tower in Qatar | 400 | 84 | 67 | 23 | N.A. | 200 cal) |
| 12 | Incheon Tower CPF) | 601 | 151 | 98 | 2 | N.A. | 43 cal) |
| 13 | Emirates Twin Towers CPF) | 355 | 56 | 93 cal) | 7 cal) | N.A. | 12 |

Note: CPF) conventional pile foundations; cal) predicted load share by calculation; N.A. = not available info

### 2.4.7 Datum Jelatek in KL, Malaysia

**Phung Duc Long (2016)** has done a case study to validate the simplified method developed for predicting the settlement of piled raft foundations. Datum Jelatek, located around 4 km from central Kuala Lumpur, Malaysia, was the project under consideration. The development includes a 12-story pedestal with retail, office, and parking bay floors, as well as four multi-story residential buildings with stories ranging from 41 to 47, as seen in Figure 2-48. The underground basement of the complex contains three floors for parking automobiles and stores. At level 24, a circular-shaped bridge joins the four towers. The distributed load on top of the podium was around 167 kPa, whereas the distributed loads in Tower A, Tower B, Tower C, and Tower D were 470.4 kPa, 475.9 kPa, 505.4 kPa, and 458.4 kPa, respectively. Figure 2-49 depicts the arrangement of the project engineers' conventional pile foundation, which used 387 piles, including 67 piles with a diameter of 0.9 m, 110 piles with a diameter of 1.2 m, and 210 piles with a diameter of 1.5 m. Conventional pile foundations with a large number of piles are frequently too safe and have too minor settlements (Phung, 2011).

Figure 2-48 : Project Datum Jelatek in KL, Malaysia (after Phung Duc Long, 2016)

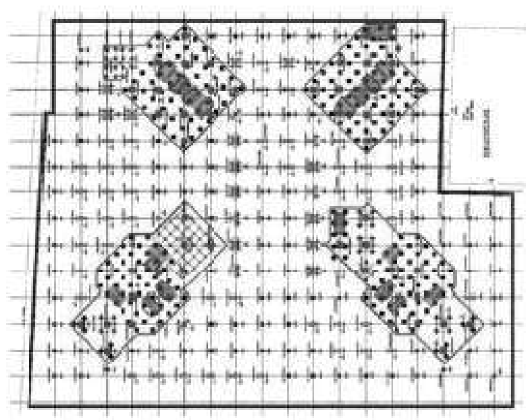

Figure 2-49 : Conventional pile foundation layout (after Phung Duc Long, 2016)

Simplified design procedure for piled footings in sand can be carried out with the following steps Phung Duc Long (2016):

1) Step 1: permissible settlement for the foundation.

2) Step 2: At the permissible settlement $s_{permissible}$ , the load taken by cap/unpiled raft, $P_{cap}$ ,is determined using any available shallow footing method, such as empirical, analytical, or numerical analysis.

3) Step 3: Estimate the load taken by the piles:

$$P_{piles} = P_{total} - P_{cap} \tag{2-72}$$

where, $P_{total}$ is the total applied load.

4) Step 4: Determine the number of piles:

$$n = P_{piles} / P_s \tag{2-73}$$

where, $P_s$ is the load carrying capacity of a single pile.

As a result of simplified method used with PLAXIS 3D, 16 piles were required for each tower A and D and 21 piles were required for each tower B and C, totaling 74 piles for the four towers, as shown in Figure 2-49. A 0.8 m thick diaphragm wall, or DW, built around the perimeter of the foundation could serve as a bearing element. The results in the case study are quite reliable since, after the number of piles was established using the simplified approach described above, the settlement of the piled raft foundation was also examined using PLAXIS 3D.